

# A previously overlooked, highly diverse early Pleistocene elasmobranch assemblage from southern Taiwan (#73574)

1

Second revision

## Guidance from your Editor

Please submit by **17 Sep 2022** for the benefit of the authors .



### Structure and Criteria

Please read the 'Structure and Criteria' page for general guidance.



### Raw data check

Review the raw data.



### Image check

Check that figures and images have not been inappropriately manipulated.

Privacy reminder: If uploading an annotated PDF, remove identifiable information to remain anonymous.

## Files

Download and review all files from the [materials page](#).

1 Tracked changes manuscript(s)  
1 Rebuttal letter(s)  
21 Figure file(s)  
4 Table file(s)



# Structure and Criteria

## Structure your review

The review form is divided into 5 sections. Please consider these when composing your review:

1. BASIC REPORTING
2. EXPERIMENTAL DESIGN
3. VALIDITY OF THE FINDINGS
4. General comments
5. Confidential notes to the editor

 You can also annotate this PDF and upload it as part of your review

When ready [submit online](#).

## Editorial Criteria

Use these criteria points to structure your review. The full detailed editorial criteria is on your [guidance page](#).

### BASIC REPORTING

-  Clear, unambiguous, professional English language used throughout.
-  Intro & background to show context. Literature well referenced & relevant.
-  Structure conforms to [PeerJ standards](#), discipline norm, or improved for clarity.
-  Figures are relevant, high quality, well labelled & described.
-  Raw data supplied (see [PeerJ policy](#)).

### EXPERIMENTAL DESIGN

-  Original primary research within [Scope of the journal](#).
-  Research question well defined, relevant & meaningful. It is stated how the research fills an identified knowledge gap.
-  Rigorous investigation performed to a high technical & ethical standard.
-  Methods described with sufficient detail & information to replicate.

### VALIDITY OF THE FINDINGS

-  Impact and novelty not assessed. *Meaningful* replication encouraged where rationale & benefit to literature is clearly stated.
-  All underlying data have been provided; they are robust, statistically sound, & controlled.
-  Conclusions are well stated, linked to original research question & limited to supporting results.



The best reviewers use these techniques

## Tip

## Example

**Support criticisms with evidence from the text or from other sources**

*Smith et al (J of Methodology, 2005, V3, pp 123) have shown that the analysis you use in Lines 241-250 is not the most appropriate for this situation. Please explain why you used this method.*

**Give specific suggestions on how to improve the manuscript**

*Your introduction needs more detail. I suggest that you improve the description at lines 57- 86 to provide more justification for your study (specifically, you should expand upon the knowledge gap being filled).*

**Comment on language and grammar issues**

*The English language should be improved to ensure that an international audience can clearly understand your text. Some examples where the language could be improved include lines 23, 77, 121, 128 – the current phrasing makes comprehension difficult. I suggest you have a colleague who is proficient in English and familiar with the subject matter review your manuscript, or contact a professional editing service.*

**Organize by importance of the issues, and number your points**

1. Your most important issue
2. The next most important item
3. ...
4. The least important points

**Please provide constructive criticism, and avoid personal opinions**

*I thank you for providing the raw data, however your supplemental files need more descriptive metadata identifiers to be useful to future readers. Although your results are compelling, the data analysis should be improved in the following ways: AA, BB, CC*

**Comment on strengths (as well as weaknesses) of the manuscript**

*I commend the authors for their extensive data set, compiled over many years of detailed fieldwork. In addition, the manuscript is clearly written in professional, unambiguous language. If there is a weakness, it is in the statistical analysis (as I have noted above) which should be improved upon before Acceptance.*

# A previously overlooked, highly diverse early Pleistocene elasmobranch assemblage from southern Taiwan

**Chia-Yen Lin** <sup>Equal first author, 1</sup>, **Chien-Hsiang Lin** <sup>Corresp., Equal first author, 1</sup>, **Kenshu Shimada** <sup>2, 3</sup>

<sup>1</sup> Biodiversity Research Center, Academia Sinica, Taipei, Taiwan

<sup>2</sup> Department of Environmental Science and Studies and Department of Biological Sciences, DePaul University, Chicago, Illinois, The United States of America

<sup>3</sup> Sternberg Museum of Natural History, Fort Hays State University, Hays, Kansas, The United States of America

Corresponding Author: Chien-Hsiang Lin  
Email address: chlin.otolith@gmail.com

The Niubu fossil locality in Chiayi County, southern Taiwan is best known for its rich early Pleistocene marine fossils that provide insights into the poorly understood past diversity in the area. The elasmobranch teeth at this locality have been collected for decades by the locals, but have not been formally described and have received little attention. Here, we describe three museum collections of elasmobranch teeth ( $n = 697$ ) from the Liuchungchi Formation (1.90–1.35 Ma) sampled at the Niubu locality, with an aim of constructing a more comprehensive view of the past fish fauna in the subtropical West Pacific. The assemblage is composed of 20 taxa belonging to 9 families and is dominated by *Carcharhinus* and *Carcharodon*. The occurrence of †*Hemipristis serra* is of particular importance because it is the first Pleistocene record in the area. We highlight high numbers of large *Carcharodon carcharias* teeth in our sample correlating to body lengths exceeding 4 m, along with the diverse fossil elasmobranchs, suggesting that a once rich and thriving marine ecosystem in an inshore to offshore shallow-water environment during the early Pleistocene in Taiwan.

# A previously overlooked, highly diverse early Pleistocene elasmobranch assemblage from southern Taiwan

Chia-Yen Lin<sup>1,#</sup>, Chien-Hsiang Lin<sup>1,#</sup>, Kenshu Shimada<sup>2,3</sup>

<sup>1</sup> Biodiversity Research Center, Academia Sinica, Taipei, Taiwan

<sup>2</sup> Department of Environmental Science and Studies and Department of Biological Sciences, DePaul University, Chicago, Illinois, USA

<sup>3</sup> Sternberg Museum of Natural History, Fort Hays State University, Hays, Kansas, USA

# Equal first author

Corresponding Author:

Chien-Hsiang Lin<sup>1</sup>

Biodiversity Research Center, Academia Sinica, Taipei, Taiwan

Email address: [chlin.otolith@gmail.com](mailto:chlin.otolith@gmail.com)

## Abstract

The Niubu fossil locality in Chiayi County, southern Taiwan is best known for its rich early Pleistocene marine fossils that provide insights into the poorly understood past diversity in the area. The elasmobranch teeth at this locality have been collected for decades by the locals, but have not been formally described and have received little attention. Here, we describe three museum collections of elasmobranch teeth (n = 697) from the Liuchungchi Formation (1.90–1.35 Ma) sampled at the Niubu locality, with an aim of constructing a more comprehensive view of the past fish fauna in the subtropical West Pacific. The assemblage is composed of 20 taxa belonging to 9 families and is dominated by *Carcharhinus* and *Carcharodon*. The occurrence of †*Hemipristis serra* is of particular importance because it is the first Pleistocene record in the area. We highlight high numbers of large *Carcharodon carcharias* teeth in our sample correlating to body lengths exceeding 4 m, along with the diverse fossil elasmobranchs, suggesting that a once rich and thriving marine ecosystem in an inshore to offshore shallow-water environment during the early Pleistocene in Taiwan.

## Introduction

The Indo-West Pacific is regarded as one of the crucial marine biodiversity hotspots in the world (Myers et al., 2000; Bellwood & Meyer, 2009). Most of the species are concentrated in the coral reef triangle area that has its northern limit extending to southern Taiwan. A remarkable 181 chondrichthyan species have been recorded in the modern fish fauna of Taiwan (Ebert et al.,

2013), approximating over 15% of the total number of global chondrichthyan species (Weigmann, 2016). Such species diversity is regarded as one of the highest biodiversity hotspots for elasmobranchs when considering the size of Taiwan (Ebert et al., 2013). However, how this remarkable chondrichthyan fauna was formed and evolved in the past are not well understood, primarily because relevant fossil records are traditionally overlooked or unstudied, despite being well-represented in the marine deposits of Taiwan. Thus, comparisons for associated fossil fauna and past biogeographic distributions are limited, particularly in the tropical-subtropical Pacific. Lin et al. (2021) highlighted the need for paleontological data for understanding the historical context of fish fauna and further recommended research potentials in the region.

In the Western Foothills of Taiwan, numerous Neogene to Quaternary strata are known to be rich in marine fossils (e.g., Ribas-Deulofeu, Wang & Lin, 2021; Lin & Chien, 2022; Lin et al., 2022). For instance, the early Pleistocene Liuchungchi Formation in the Niubu area, Chiayi County, southwestern Taiwan is of particular research interest due to its abundance and diversity of marine fauna. This fauna includes mollusks (Hu, 1989; Xue, 2004), crabs (Hu, 1989; Hu & Tao, 1996, 2004; Xue, 2004), sea urchins (Hu, 1989; Xue, 2004), whale barnacles (Buckeridge, Chan & Lee, 2018), teleost bones (Tao, 1993) and otoliths (Lin et al., 2018), and elasmobranch teeth (Xue, 2004). Fossils from this region were collected by the late W.-J. Xue during the 1980s-2000s, and currently this large and diverse collection (over 3,000 specimens) is mainly deposited in the Chiayi Municipal Museum, Chiayi City, Taiwan (CMM). There is a considerable number of elasmobranch teeth from Xue's collection that were reported by Xue (2004) in the form of photographic atlas without descriptions, and another collection donated by Prof. Hsi-Jen Tao (National Taiwan University) to the Biodiversity Research Museum, Academia Sinica, Taipei, Taiwan (BRMAS) is available. An additional small collection is also deposited in the National Taiwan Museum (NTM). The purpose of this present study is to properly document the occurrences of these elasmobranch fossils from the Liuchungchi Formation at the Niubu locality based on these collections and few newly collected specimens. The diverse association of teeth provides opportunities for obtaining a more complete view of the Pleistocene elasmobranch fauna in the rarely explored subtropical West Pacific.

## Geological setting

Since the late Miocene, the island of Taiwan was gradually uplifted by the Penglai orogeny—the collision between the Chinese continental margin and the Luzon Arc—and, subsequently, a series of subsiding foreland basins were formed in western Taiwan (Ho, 1976; Suppe, 1984; Lundberg et al., 1997; Lin & Watts, 2002; Nagel et al., 2013; Chen, 2016). These foreland basins gradually developed from north to south accumulating clastic sediments (Ho, 1967; Covey, 1984; Teng, 1990), and in the south the basins have high deposition rates (700–900 m/Ma) due to a deeper depositional environment (Chen, Huang & Yang, 2011). Thus, the depositional sequences reflect sea-level changes during the Quaternary that followed the 100 ky orbit eccentricity cycles (Chen, Huang & Yang, 2011; Chen, 2016). Meanwhile, thick pre-orogenic

and synorogenic sediments infilling the foreland basin were squeezed and uplifted, which formed the 7–9 km Miocene to Pleistocene strata in the Western Foothills (Yu & Chou, 2001; Nagel et al., 2013).

The Liuchungchi Formation in the Niubu area, Chiayi County is exposed along the Bazhang River (Fig. 1B). Four successive formations are exposed from east to west: the Liuchungchi, Kanhsialiao, Erhchungchi, and Liushuang formations (Stach, 1957; Chou, 1975; Chen, Huang & Yang, 2011; Chen, 2016; Fig. 1B, C). The age of the Liuchungchi Formation is 1.90–1.35 Ma (Chen, 2016), with a deposition rate of about 700 m/Myr in the lower section and 1,100 m/Myr upsection, the maximum thickness of the formation is 760 m (Chen, Huang & Yang, 2011). The Liuchungchi Formation is composed of dozens of depositional sequences, each representing a 41 ky climate cycle (Chen, Huang & Yang, 2011; Chen, 2016). The depositional environment can be divided into two distinct sections, with the lower sequence composed of thick sandstone with cross bedding, parallel bedding, and strong bioturbation reflecting shoreface to the offshore transition zone, and the upper sequence composed of interbeds of sandstone and shale and storm deposits in the form of sandstone, indicating the inner offshore (Chen, Huang & Yang, 2011; Chen, 2016).

## Materials & Methods

The fossil site is located in the Niubu area, Chiayi County, southwestern Taiwan, about 15 km east of Chiayi City (Fig. 1A). The layers containing fossils are exposed along the Bazhang River, just downstream of a dam near a high-voltage tower, where they are readily accessible during the dry seasons (winter) when the water level is low (Supplemental Fig. S1). Fossil mollusks are very abundant in several of the condensed layers, as well as fragments of crabs, sea urchins, and teleost fish bones (Fig. 2A). Fossil shark teeth are rare based on both surface collecting and bulk sampling conducted during our several field trips in 2018–2022. Bulk sediment samples of over 830 kg (Sites 1–3 in Fig. 2B) were sieved (500- $\mu$ m mesh) from the loosely cemented siltstone, yielding a large number of otoliths (Lin et al., unpublished data), but only one shark tooth and two ray teeth. We note the discrepancy in the numbers of elasmobranch specimens in museum collections and our field surveys, which can be explained by the fact that the larger sample sizes in museum collections primarily reflect collecting based on chance occurrences of shark teeth over the past 3–4 decades, compared to collecting based on our limited number of field surveys. Moreover, the initial purpose of the bulk sampling was for collecting teleost otoliths instead of elasmobranch teeth due to their abundance.

The upstream area of Bazhang River contains strata older than the Liuchungchi Formation; these include the Neogene Tangenshan Sandstone and Yenshuikeng Shale, which are exposed approximately 1 km east of a weir (Figs. 1, 2), with an elevation of more than 300 m above the level of our sampling sites. Both stratigraphic units are composed of consolidated sandstones with some marine fossils such as mollusks, which are different from the fine, unconsolidated

siltstones of the Liuchungchi Formation. After storms and rainy seasons, numerous blocks of sandstone from these older strata can be found along the riverbed of the Bazhang River (Supplemental Fig. S1). These blocks are lithologically distinct and confined to areas below our sampling sites. Although we consider our material as early Pleistocene and that the mixing of older Neogene fossils with our specimens is improbable, we cannot rule entirely that certain worn material (e.g., Myliobatiformes) is not reworked. Further geochemical analysis (e.g., Sr-isotope, Kocsis et al., 2021, 2022) would help determine the extent of the reworking.

The BRMAS, CMM, and NTM collections analyzed here were collected from the surface exposures of the Niubu locality without bulk-sampling of sediments; however, the exact stratigraphic horizons and detailed lithology within the Liuchungchi Formation for each specimen are not known. Stacked images of teeth were taken and measurements of crown height (CH), mesial crown edge length (MCL), and basal crown width, (BCW) were noted whenever possible. Specimens from the BRMAS are registered under ASIZF, CMM under CMM F, and those in the NTM are under NTM I. Because the Pleistocene is relatively close to modern times, the morphology of elasmobranch teeth has not changed much from that time to the present. Therefore, identifications of these fossil teeth were conducted by comparing them with teeth of extant taxa.

The diversity of our elasmobranch assemblage was compared with other Pleistocene assemblages to highlight its significance within the associated spatio-temporal context. Taxonomic composition and abundance data from the early Pleistocene temperate assemblages of Japan (Karasawa, 1989; Kawase & Nishimatsu, 2016; Tanaka & Taru, 2022) and tropical records from Java (Koumans, 1949; Yudha et al., 2018) and Sulawesi (Hooijer, 1954) were compared. We calculated diversity indices, including species richness (number of species recorded), Shannon's entropy (Shannon, 1948), Simpson's diversity index (Simpson, 1949), and Fisher's alpha (Fisher et al., 1943) for a general comparison.

## Systematic Paleontology

A summary of taxa and their numeric abundance are listed in Table 1. The elasmobranch assemblage contains 697 teeth, consisting of 9 families and 20 taxa. The classification scheme follows that of Nelson, Grande & Wilson (2016), except for the family Galeocerdonidae, which we follow Fricke, Eschmeyer & Van der Laan (2022). General morphological terminology follows that of Compagno (1984, 2002), Purdy et al. (2001), Shimada (2002), Purdy (2006), Cappetta (2012), and Ebert et al. (2013). The synonymy list is limited to relevant records from Taiwan (Huang, 1965; Uyeno, 1978; Hu & Tao, 1993; Xue, 2004; Tao & Hu, 2008).

Class Chondrichthyes Huxley, 1880

Order Lamniformes Berg, 1958

Family Carchariidae Müller & Henle, 1838



Genus *Carcharias* Blainville, 1816  
*Carcharias taurus* Rafinesque, 1810  
 (Fig. 3)  
 1978 *Odontaspis* sp.; Uyeno, pl. 1, fig. 5.

**Referred specimens:** n = 2: ASIZF0100320, CMM F0204.

**Description:** CH = 12.92–16.83 mm; MCL = 12.18–15.54 mm; BCW = 7.07–7.84 mm. The teeth are characterized by a slender, dagger-like main cusp and a single pair of small lateral cusplets. The crown exhibits no serrations. The lingual protuberance of the root is prominent.

**Remarks:** The teeth of *Carcharias taurus* are similar to those of *Odontaspis noronhai* and *O. ferox* by having a slender main cusp and lateral cusplet. However, the lateral cusplets of *Odontaspis* are more pronounced than those of *C. taurus*, including the fact that teeth of *O. ferox* typically exhibit multiple pairs of lateral cusplets.

Family Lamnidae Bonaparte, 1835  
 Genus *Carcharodon* Smith, 1838  
*Carcharodon carcharias* (Linnaeus, 1758)  
 (Fig. 4)

1978 *Carcharhinus* sp.; Uyeno, pl. 1, fig. 4, pl. 2, fig. 7.  
 1978 *Carcharodon carcharias*; Uyeno, pl. 3, figs. 12, 13.  
 2004 Elasmobranchii indet.; Xue, pl. 1, figs. 1–6, pl. 2, figs. 1–7, pl. 3, figs. 1, 2–7, pl. 7 fig. 2.

**Referred specimens:** n = 55: ASIZF0100322–0100346, 0100435, 0100465, 0100530. CMM F0001–F0005, F0007–F0010, F0012–F0022, F0210, F0212, F2824, F2825, F2830, NTM I01122, I01123.

**Description:** CH = 6.76–41.03 mm; MCL = 9.61–45.68 mm; BCW = 8.74–37.09 mm. The upper teeth (Fig. 4A–N) are broad and triangular. The cutting edge of both mesial and distal sides is almost straight with coarse serrations. The labial face of the crown is flat and the lingual face is convex, where the crown is erect and symmetric to slightly distally inclined depending on tooth positions. The root is slightly arched, and the nutritive foramina and transverse groove are not prominent or absent. The lower teeth (Fig. 4O–X) have a more robust but narrower serrated crown and bilobate roots with a rounded lingual face compared to the upper teeth.

**Remarks:** The genus *Carcharodon* is represented by three species: †*C. hastalis*, †*C. hubbelli*, and *C. carcharias*. Whereas *C. hastalis*, which was traditionally placed in the genus *Isurus* or †*Cosmopolitodus*, lived through the Miocene and early Pliocene, †*C. hubbelli* in the late Miocene and *C. carcharias* in the early Pliocene–Recent form a single lineage of chronospecies by developing serrations on their teeth (Ehret et al., 2012). The specimens described in this present paper exhibit well-developed serration consistent with teeth of *C. carcharias* (e.g.,

Hubbell, 1996), and not like the teeth of *C. hubbelli* with weak serrations (Ehret et al., 2012). They include the largest dental remains among all the shark tooth specimens described in this paper.

Genus *Isurus* Rafinesque, 1810

*Isurus oxyrinchus* Rafinesque, 1810

(Fig. 5)

?1965 *Isurus hastalis*; Huang, pl. 22, figs. 12–14.

1993 *Isurus hastalis*; Hu & Tao, pl. 24, figs. 6, 8.

2004 Elasmobranchii indet.; Xue, pl. 5, fig. 3, pl. 8, fig. 4.

2008 *Isurus* sp.; Tao & Hu, pl. 2, figs. 1–2.

**Referred specimens:** n = 6: ASIZF0100317–0100319, 0100321, CMM F0242, NTM I01131\_1.

**Description:** CH = 9.86–27.81 mm; MCL = 12.21–26.89 mm; BCW = 9.31–9.96 mm. The anterior teeth have a slender, dagger-like, unserrated crown that is erect or lingually curved with an apical labial flexure (Fig. 5A–H). The root, if preserved, has two rather narrow lobes with a moderately tight basal concavity. The lateral teeth have a flatter and broader, distally curved, unserrated crown with a short but mesiodistally wide root (Fig. 5I, J).

**Remarks:** Two extant species of *Isurus* are known: *I. oxyrinchus* and *I. paucus*. *Isurus oxyrinchus* has a more elongated and more labially curved crown than *I. paucus* (Whitenack & Gottfried, 2010). The teeth of *I. oxyrinchus* are also similar to those of *Carcharias taurus*, but the teeth of *C. taurus* have a pair of lateral cusplets that is absent in the teeth of *I. oxyrinchus* (Wilmers, Waldron & Bargmann, 2021). Huang (1965) reported a tooth of †*I. hastalis* (= *Carcharodon hastalis*; see above) from the Pleistocene Cholan Formation in Hsinchu, northern Taiwan; however, this species identification is questionable and the whereabouts of the specimen is unknown for verification.

Order Carcharhiniformes Compagno, 1973

Family Hemigaleidae Hasse, 1878

Genus *Hemipristis* Agassiz, 1835

†*Hemipristis serra* Agassiz, 1843

(Fig. 6)

1978 *Hemipristis serra*; Uyeno, pl. 1, fig. 2.

2004 *Hemipristis* sp.; Xue, pl. 5, figs. 1, 2, 5, 6, 7.

2004 Elasmobranchii indet.; Xue, pl. 5, fig. 5, pl. 7, figs. 3, 5, pl. 9, figs. 6, 7.

2008 *Hemipristis serra*; Tao & Hu, pl. 6, fig. 1.

**Referred specimens:** n = 7: ASIZF0100460–0100462, CMM F0232, F2826, F2827, NTM I01131\_2.

**Description:** CH = 5.21–30.81 mm; MCL = 8.73–41.38 mm; BCW = 6.50–36.59 mm. All collected specimens of this taxon represent upper teeth that are characterized by a distally inclined, broad triangular crown, and a mesiodistally separated bilobate root. Coarse serrations are present along the distal cutting edge, whereas serrations along the mesial cutting edge are finer. The root has a prominent lingual protuberance with a deep nutritive groove, and has a notch-like shallow basal concavity. The crown overhangs the root, and the crown-root boundary, especially on the lingual face, is strongly arched.

**Remarks:** As presumed sister species, the teeth of extinct †*Hemipristis serra* and extant *H. elongata* are similar. However, compared to †*H. serra*, teeth of *H. elongata* possess a more gracile crown, a longer apex without serration, and a narrower root (Smith, 1957; Purdy et al., 2001). The Pleistocene records of †*H. serra* are rare globally compared to its Neogene records (Hooijer, 1954, 1958; Yabumoto & Uyeno, 1994; Carrillo-Briceño et al., 2015; Ebersole, Ebersole & Cicimurri, 2017; Boessenecker, Boessenecker & Geisler, 2018).

Family Carcharhinidae Jordan & Evermann, 1896

Genus *Carcharhinus* Blainville, 1816

**Remarks:** The identification based on teeth below the genus level is difficult for *Carcharhinus* (Compagno, 1984, 1988; Purdy et al., 2001; Naylor & Marcus, 1994; Marsili, 2006; Voigt & Weber, 2011; Ebert, Dando & Fowler, 2021). Most of the upper teeth are triangular with crowns inclining distally. In different species, the crown varies from narrow to broad, has smooth to coarsely serrated cutting edges, variable notch angles on distal cutting edges, and the straight to convex mesial cutting edge. At least nine species of *Carcharhinus* are recorded in the collections: *C. altimus*, *C. amboinensis*, *C. leucas*, *C. limbatus*, *C. longimanus*, *C. obscurus*, *C. plumbeus*, *C. sorrah*, and *C. tjtutjot*. See remarks below for comparisons among other similar-looking species.

*Carcharhinus altimus* (Springer, 1950)

(Fig. 7)

**Referred specimens:** n = 17: ASIZF0100357, 0100359, 0100362, 0100363, 0100365, CMM F0080, F0101, F0113, F0134, F0214, F0224, F0293, F0304, F0322, F0363, TNM I01125, I01129\_1.

**Description:** CH = 4.55–9.82 mm; MCL = 7.91–12.72 mm; BCW = 7.10–10.92 mm. The specimens examined in this study consist only of upper teeth. The crown of the upper teeth is finely serrated and varies in shape from a tall triangle to distally oblique. There is a notch on the distal cutting edge, whereas a slight constriction occurs on the lower part of the mesial cutting edge. The root is arched and has a nutritive groove. The roots of some specimens are not well-

preserved (Fig. 7A, B, E, F, I–L), but where well-preserved (Fig. 7C, D, G, H), it is arched and exhibits a nutritive groove on the lingual face.

**Remarks:** Teeth of *Carcharhinus altimus* and *C. plumbeus* are similar. However, those of *C. altimus* exhibit a distally bent apex unlike those of *C. plumbeus* that show an apically directed apex (Figs. 7 vs. 13).

*Carcharhinus amboinensis* (Müller & Henle, 1839)  
(Fig. 8)

**Referred specimens:** n = 5: ASIZF0100366, 0100368, 0100369, CMM F0209, F0229.

**Description:** CH = 6.88–8.95 mm; MCL = 9.28–14.74 mm; BCW = 9.16–16.86 mm. The triangular crown is broad and exhibits coarse serrations although the serrations become smaller towards the apex. A prominent tooth neck is present between the crown and root on the lingual face. There is a notch on the distal cutting edge, whereas the mesial cutting edge is nearly straight. The bilobed root is gently arched and has a nutritive groove on the lingual face.

**Remarks:** Teeth of *Carcharhinus amboinensis*, *C. leucas*, and *C. longimanus* are very similar (Marsili, 2006; Voigt & Weber, 2011). However, the angle of the notch on the distal cutting edge of *C. longimanus* is larger than *C. leucas* and *C. amboinensis*. Compared to the teeth of *C. leucas*, the upper teeth of *C. amboinensis* are somewhat broader, the crowns are generally lower and more distally curved, and their distal heel is more pronounced and is closer to the base of the crown (Kocsis et al., 2019).

*Carcharhinus leucas* (Valenciennes, 1839)  
(Fig. 9)

?1965 *Carcharhinus gangeticus*; Huang, pl. 22, figs. 19, 20.  
2004 Elasmobranchii indet.; Xue, pl. 3, fig. 2, pl. 4, fig. 3, pl. 7, fig. 7, pl. 9, fig. 4.

**Referred specimens:** n = 71: ASIZF0100390, 0100393–0100398, 0100400–0100404, 0100411, 0100419, 0100424, 0100425, 0100481, CMM F0154, F0155, F0157, F0159, F0162, F0163, F0165–F0168, F0170–F0175, F0180, F0183, F0186–F0188, F0190, F0192, F0198–F0201, F0205, F0206, F0221, F0222, F0227, F0231, F0240, F0244, F0246, F0249, F0288, F0290, F0297, F0299, F0301, F0317, F0319, F0321, F0328, F0332, F0334, F0341, F0342, F0348, F0354, F0362, NTM I01130\_2.

**Description:** CH = 4.87–18.68 mm; MCL = 7.97–21.69 mm; BCW = 8.73–30.56 mm. The teeth of *Carcharhinus leucas* are generally robust. The crown of the upper teeth (Fig. 9A–P) is broad and triangular with a slight distal inclination. The middle of the distal cutting edge is concave, forming a weak notch, whereas the mesial cutting edge is straight to slightly convex. Both cutting edges are coarsely serrated, but the sizes of serrations are smaller at the base and apex of the crown than those in the middle. The boundary between the crown base and root on the

lingual face displays a V-shape tooth neck. The bilobate root is arched and displays a weak nutritive groove on the lingual face (Fig. 9A–H, K, L). The lower teeth (Fig. 9Q, R), that have fine serrations, are labiolingually thicker and mesiodistally narrower than the upper teeth. **Remarks:** Marsili (2006) described the crown of *Carcharhinus longimanus* as larger, more elongate and possessing a straighter root margin compared to that of *C. leucas*. In addition, based on the images of *Carcharhinus* by Garrick (1982) and Voigt & Weber (2011), we find some other slight differences in tooth morphology between the two species. For example, the angle on the distal cutting edge of the upper teeth in *C. longimanus* is larger than that in *C. leucas*, making the crown of *C. leucas* incline more distally than that in *C. longimanus*. In addition, the tooth shape of *C. leucas* is close to a wide-bottom triangle, whereas that of *C. longimanus* forms a taller triangle. Furthermore, the lower teeth of *C. leucas* tend to exhibit a stronger demarcation between the main cusp and mesial and distal heels than those of *C. longimanus* with a smoother cusp-heel transition.

*Carcharhinus limbatus* (Valenciennes, 1839)  
(Fig. 10)

1978 *Carcharhinus* sp.; Uyeno, pl. 3, fig. 14.  
2004 Elasmobranchii indet.; Xue, pl. 8, fig. 5.

**Referred specimens:** n = 40: ASIZF0100467–0100480, 0100482, 0100483, CMM F0056, F0111, F0216, F0217, F0234, F0236–F0238, F0286, F0289, F0291, F0295, F0306, F0307, F0310, F0368–F0373, NTM I01127, I01133\_2, I01134\_2.

**Description:** CH = 7.70–9.31 mm; MCL = 10.02–13.26 mm; BCW = 10.26–14.70 mm. Our specimens consist only of upper teeth. The teeth of *C. limbatus* are serrated and are characterized by a narrow cusp that is erect to slightly oblique distally with a mesiodistally wide crown base. The serrations near the crown base are coarser than those towards the apex. The root is apicobasally shallow. Its base is straight to slightly arched with a prominent deep nutritive groove that forms a notch along the root base.

**Remarks:** Although similar, teeth of *Carcharhinus limbatus* can be distinguished from those of *C. amblyrhynchoides*, *C. brachyurus* and *C. brevipinna*. Unlike the teeth of *C. limbatus*, the serrations on the cutting edges tend not to continue to the crown base in *C. amblyrhynchoides*, are absent or weak in *C. brevipinna*, and in *C. brachyurus*, the apex is more pointed and more distally directed than in *C. limbatus* (Garrick, 1982; Voigt & Weber, 2011). In addition, the crowns of *C. limbatus* have a narrow, erect cusp with a sharp transition to a broad crown base that is distinct from all other congeneric specimens examined. The teeth of *C. limbatus* and *C. amblyrhynchoides* are, however, very difficult to distinguish. Kocsis et al. (2019) noted a narrower crown with finer serrations in *C. limbatus*, but this character is not clear in our specimens. Currently, no records of *C. amblyrhynchoides* have been reported in Taiwan (Ebert et al., 2013; Shao, 2022); therefore, we tentatively assign these specimens to *C. limbatus*.

*Carcharhinus longimanus* (Poey, 1861)  
(Fig. 11)

1965 *Carcharhinus gangeticus*; Huang, pl. 22, figs. 21, 22.  
2004 Elasmobranchii indet.; Xue, pl. 4, fig. 4, pl. 7, fig. 6, pl. 9, fig. 1.

**Referred specimens:** n = 36: ASIZF0100370, 0100371, 0100373–0100382, 0100391, 0100392, 0100421, 0100422, 0100428, 0100466, CMM F0006, F0011, F0087, F0151, F0153, F0156, F0158, F0182, F0189, F0194, F0195, F0197, F0223, F0248, F0287, F0294, NTM I01128, NTM I01130.

**Description:** CH = 10.23–15.93 mm; MCL = 13.51–22.08 mm; BCW = 13.20–21.69 mm. The crowns of the upper teeth (Fig. 11A–P) are broad, triangular, and coarsely serrated. The distal cutting edge is weakly concave, whereas the mesial cutting edge is nearly straight. The crown base on the lingual side is deeply concave and is accompanied basally by a narrow tooth neck and a deep bilobate root with a shallow nutritive groove. The lower teeth (Fig. 11Q–T) are thicker and narrower than the upper teeth, they also have fine serrations on the cutting edges. The boundary between the crown base and root on the lingual side is also deeply concave with a V-shaped tooth neck.

**Remarks:** See remarks under *Carcharhinus leucas*.

*Carcharhinus obscurus* (Lesueur, 1818)  
(Fig. 12)

2004 Elasmobranchii indet.; Xue, pl. 4, fig. 7.

**Referred specimens:** n = 25: ASIZF0100372, 0100383–0100389, 0100399, CMM F0123, F0143, F0148, F0160, F0164, F0176–F0179, F0181, F0184, F0196, F0208, F0338, F0353, NTM I1132\_3.

**Description:** CH = 5.04–15.14 mm; MCL = 7.57–21.61 mm; BCW = 9.56–20.96 mm. The specimens in this study consist only of upper teeth. They are broad and triangular with coarse serrations, although the serrations tend to become finer apically. The mesial cutting edge is overall slightly convex with a marked distally directed apex. The distal cutting edge has a relatively deep notch, but the degree of the angle varies based on tooth position within the dentition. The crown base on the lingual side is moderately concave and is accompanied by a prominent tooth neck and a relatively robust bilobed root that has a shallow nutritive groove.

**Remarks:** The crown of *Carcharhinus obscurus* is mesiodistally broad and typically exhibits coarse serrations along the middle section of both cutting edges, a feature for separating all other congeneric specimens in the present study.

*Carcharhinus plumbeus* (Nardo, 1827)

(Fig. 13)

**Referred specimens:** n = 51, ASIZF0100405–0100410, 0100412, 0100429, CMM F0074–F0077, F0079, F0086, F0088, F0091, F0096, F0100, F0106, F0115, F0124, F0144, F0146, F0169, F0225, F0228, F0292, F0302, F0316, F0318, F0320, F0325–F0327, F0330, F0331, F0333, F0335, F0337, F0346, F0347, F0349, F0350, F0352, F0356, F0360, F0361, F0364, F0365, F0367, NTM I01124.

**Description:** CH = 6.28–12.17 mm; MCL = 7.81–17.06 mm; BCW = 7.48–13.39 mm. The teeth that are referred to this species are all upper teeth. They are triangular with a slight distal inclination and with fine serrations. The mesial cutting edge is nearly straight, whereas the distal cutting edge tends to form a shallow notch close to the crown base. The root is bilobate and arched, and a shallow nutritive groove is present on the lingual face.

**Remarks:** The crown of *Carcharhinus plumbeus* is narrower and more elongate than that of *C. leucas*, *C. longimanus*, *C. obscurus*, and *C. amboinensis*, but it is wider than that of *C. altimus*.

*Carcharhinus sorrah* (Valenciennes, 1839)

(Fig. 14)

**Referred specimens:** n = 11: ASIZF0100418, CMM F0117, F0119, F0122, F0126, F0129, F0135, F0140, F0303, F0343, F0344.

**Description:** CH = 4.39–5.80 mm; MCL = 5.55–9.82 mm; BCW = 4.03–9.85 mm. All teeth identified to this species are represented by upper teeth. Their crowns exhibit finely serrated triangular cusps that strongly incline distally along with a coarsely serrated, relatively broad distal heel. The apex is narrow and may be slightly recurved apically (Fig. 14E–H). The serrations on the distal heel become smaller distally, where finer secondary serrations are observed on one or two of the mesial-most serrations. Well-preserved specimens exhibit a strong nutritive groove on the lingual face that forms a notch along the root base.

**Remarks:** According to Voigt & Weber (2011), the crown of the upper teeth in *Carcharhinus sorrah* is high, and its distal cutting edge is deeply notched. These features are seen in our specimens; however, the description of the serrations in Voigt & Weber (2011) differs. The serrations on the central part of the mesial cutting edges are coarser in Voigt & Weber (2011), whereas in our specimens, the coarsest serrations are on the basal part of the mesial cutting edges. Furthermore, the main cusp and coarse serrations in our specimens are farther apart than those figured by Voigt & Weber (2011). The teeth of *C. tjutjot* and *C. sorrah* are both characterized by a coarsely serrated distal heel, but the teeth of *C. tjutjot* differ from those of *C. sorrah* by having fewer but larger serrations forming a distal heel (Figs. 14 vs. 15).

*Carcharhinus tjutjot* (Bleeker, 1852)

(Fig. 15)

**Referred specimens:** n = 19: ASIZF0100413–0100417, CMM F0116, F0136–F0138, F0142, F0296, F0298, F0323, F0324, F0339, F0345, F0357, F0376, F0377.

**Description:** CH = 4.25–5.82 mm; MCL = 6.03–9.01 mm; BCW = 5.61–7.94 mm. The specimens of this species described here are all represented by upper teeth. They have a robust, distally inclined, triangular cusp with a small distal heel consisting of coarse serrations that rapidly diminish in size distally. The strongly inclined mesial cutting edge is relatively straight, where the apex may slightly recurve apically and serrations become slightly coarser towards the base. Finer secondary serrations are observed on the first and possibly second mesial-most serrations on the distal heel. The root is weakly bilobate and the root base is nearly straight. Well-preserved specimens show a shallow nutritive groove on the lingual face of the root.

**Remarks:** The teeth of *Carcharhinus sealei*, *C. dussumieri*, *C. coatesi*, and *C. tjtjt* are very similar (White, 2012). The difference between species is related to their serrations. The serrations of *C. sealei* are present only on the basal half of the mesial cutting edge, whereas the distal cutting edge, including the distal heel, is smooth (White, 2012). Cutting edges of teeth in *C. coatesi* have fine to coarse serrations, but the distal heel is smooth. In *C. dussumieri*, both cutting edges, including the distal heel, have evenly-sized coarse serrations. The teeth of *C. tjtjt* also have evenly-sized serrated cutting edges, including the distal heel. *Carcharhinus dussumieri* and *C. tjtjt* have long been misidentified due to their similar appearance, but *C. dussumieri* is now considered a West Indian species distributed from the Persian Gulf to India, whereas *C. tjtjt* is distributed from Indonesia to Taiwan (White, 2012).

Genus *Rhizoprionodon* Whitley, 1929  
*Rhizoprionodon acutus* (Rüppell, 1837)  
(Fig. 16)

Referred specimens: n = 8: ASIZF0100463, 0100464, CMM F0110, F0120, F0121, F0130, F0131, F0218.

**Description:** CH = 3.97–5.35 mm; MCL = 6.22–10.82 mm; BCW = 7.68–10.69 mm. The upper teeth of this species have a crown that is strongly inclined distally and is accompanied by a low distal heel (Fig. 16A–H). Both cutting edges, including the distal heel, are smooth or exhibit fine irregular serrations. The mesial cutting edge is overall straight, whereas the junction between the cusp and distal heel is deeply notched. A deep nutritive groove is present on the lingual side of the root that continues to the root base. The root is low with little to no basal concavity. ASIZF0100464 (Fig. 16I, J) is a lower tooth, with a crown that is unserrated and more gracile than the upper teeth with a concave mesial cutting edge. The root morphology is similar to that of lower teeth.

**Remarks:** The teeth of *Rhizoprionodon acutus* are serrated in adults (Compagno, 1984). In our specimens, the serrations are absent, indicating immature individuals. Distinguishing between the teeth of *R. acutus* and *R. oligolinx* is difficult, where both have very fine irregular serrations.



However, due to the questionable distribution of *R. oligolinxi* in Taiwan (Ebert et al., 2013; Froese & Pauly, 2022), we tentatively assign these specimens to *R. acutus*.

Family Galeocerdonidae *sensu* Ebersole, Cicimurri & Stringer, 2019

Genus *Galeocerdo* Müller & Henle, 1837

*Galeocerdo cuvier* (Péron & Lesueur, 1822)

(Fig. 17A–H)

?1965 *Galeocerdo aduncus*; Huang, pl. 22, figs. 10, 11.

?1978 *Galeocerdo aduncus*; Uyeno, pl. 1, fig. 3.

2004 Elasmobranchii indet.; Xue, pl. 6, figs. 1–7, pl. 8, fig. 6.

**Referred specimens:** n = 7: ASIZF0100459, CMM F0213, F0215, F0245, F2823, F2829, NTM I01121.

**Description:** CH = 12.27–17.72 mm; MCL = 17.37–26.88 mm; BCW = 18.10–28.05 mm. The teeth of *G. cuvier* are characterized by a coarsely serrated crown with a cusp that strongly curves distally and a prominent distal heel demarcated by a deep notch with an approximately 90 degrees angle along the distal cutting edge. Fine secondary serrations are present on the coarser primary serrations (Fig. 17E, H). The serrations on the distal heel in ASIZF0100459 (Fig. 17F, G) are weak and the width to crown height ratio suggests this tooth represents a posterior position. CMM F0245 and CMM F0215 are anterior teeth with well-marked serrations (Fig. 17A–D).

**Remarks:** Five extinct species and one extant species of *Galeocerdo* are considered valid: the Eocene †*G. clarkensis* and †*G. eaglesomi*, Oligocene–late Miocene †*G. aduncus*, Miocene †*G. mayumbensis*, Pliocene †*G. capellini*, and the Pleistocene–Recent *G. cuvier* (Purdy et al., 2001; Türtscher et al., 2021). The specimens described here are identified as *G. cuvier*, particularly because of the presence of secondary serrations (Cigala-Fulgosi & Mori, 1979; Türtscher et al., 2021). Huang (1965) reported a questionable occurrence of †*G. aduncus* from the Pleistocene Cholan Formation in Hsinchu, northern Taiwan, however we consider the specimen lost. Uyeno (1978) reported another occurrence of †*G. aduncus* from the poorly constrained Plio-Pleistocene strata along the Tsailiao River in Tainan, southwestern Taiwan (as Miocene to Pleistocene in Uyeno, 1978). Although Uyeno’s collection was deposited in the NTM, we were not able to locate the specimen of †*G. aduncus* in the collection. Nevertheless, although the whereabouts of the specimen is uncertain, it is interpreted here to have also belonged to *G. cuvier*.

Family Sphyrnidae Bonaparte, 1840

Genus *Sphyrna* Rafinesque, 1810

*Sphyrna lewini* (Griffith & Smith, 1834)

(Fig. 17I–L)

?1978 *Sphyrna* sp.; Uyeno, pl. 2, fig. 8

**Referred specimens:** n = 2: CMM F0235, F0312.

**Description:** CH = 4.64–6.85 mm; MCL = 7.51–11.17 mm; BCW = 7.19–10.53 mm. The tooth crown of *S. lewini* is characterized by a slender, distally inclined cusp with a narrow, mesially extended base separated by a slight concavity along the mesial cutting edge and a low distal heel demarcated by a deep notch. Both cutting edges are smooth without serrations. The root is low and its base is straight. It has a deep nutritive groove on the lingual side and extends to the root base.

**Remarks:** The teeth of *Sphyrna lewini* are most similar to *S. macrorhynchus* and *Loxodon macrorhinus*, but a slight concavity is present on the base of the mesial cutting edge in *S. lewini*, whereas the edge is almost straight in the latter two species (Ebert et al., 2013).

Order Myliobatiformes Compagno, 1973  
Family Dasyatidae Jordan & Gilbert, 1879  
Dasyatidae indet.  
(Fig. 18)

**Referred specimens:** n = 2: ASIZF0100590, 0100591.

**Description:** The specimens are roughly hexagonal with a globular, thick crown and a well-divided bilobed root that is smaller than the crown and extends ventrally. The crown in both specimens is flat, but the specimen ASIZF0100590 (Fig. 18A–D) has blunt, rounded corners compared to ASIZF0100591 (Fig. 18E–H).

**Remarks:** The teeth referred to this taxon may belong to the genus *Dasystis* or *Himantura*, but because teeth of dasyatid taxa are highly variable in morphology, including sexual dimorphism and differences in ornamentation pattern (Taniuchi & Shimizu, 1993; Kajiura & Tricas, 1996; Herman, Hovestadt-Euler & Hovestadt, 1998, 1999, 2000), we refer our material simply to Dasyatidae indet. Uyeno (1978) reported teeth of *Dasystis* sp. from the Miocene to Pleistocene of Taiwan. However, whether our specimens are conspecific with Uyeno's (1978) specimens cannot be ascertained.

Family Aetobatidae Agassiz, 1858  
Genus *Aetobatus* Blainville, 1816  
*Aetobatus* sp.  
(Fig. 19)

**Referred specimens:** n = 58: ASIZF0100549–0100580, CMM F0380, F0382, F0388, F0395, F0399–0409, F0412, F2848–F2850, F2852–F2854, NTM I01116, I01117, I01119, I01120.

**Description:** Teeth of *Aetobatus* are characterized by strongly extended roots on the lingual (posterior) side and the arcuate crown in apical view with a flat occlusal surface. The crown

overhangs the root on the labial (anterior) side and the root is more prominent than the crown on the lingual side. Both lingual and labial crown faces have fine vertical grooves as ornamentation. The root is polyaulocorhizous, consisting of anteroposteriorly oriented, densely packed, vertical lamellar plates.

**Remarks:** Five species of Myliobatidae (one *Aetobatus*, three *Aetomylaeus*, and one *Myliobatis*) are known from Taiwan (Ebert et al., 2013). All of which have grinding-type dental plates but each with different shapes and forms. The upper medial teeth of *Aetobatus ocellatus* are straight and elongate but slightly distally deflected towards the lingual side; its lower teeth are strongly arched towards the labial side. Considerable ontogenetic morphological change in dental plates is known in *Aetomylaeus* (Hovestadt & Hovestadt-Euler, 2013). Both upper and lower dental plates of adult *Aetomylaeus* are similar to the upper teeth of *Aetobatus*. Unlike adult individuals that have a single row of medial teeth, juveniles of *Aetomylaeus* have one medial, two lateral, and one posterior tooth row (Hovestadt & Hovestadt-Euler, 2013). The hexagon shape of medial teeth is very similar to those of juvenile *Myliobatis* (Hovestadt & Hovestadt-Euler, 2013). Teeth of *Aetobatus* have weak ornaments on the labial and lingual crown, but in *Aetomylaeus*, beaded ridges with reticulated and pitting patterns are observed (Ebersole, Cicimurri & Stringer, 2019). Moreover, *Aetobatus* has teeth with a strong arched appearance than other myliobatid genera (see also remarks under *Myliobatis* sp.).

Family Myliobatidae Bonaparte, 1835

Genus *Myliobatis* Cuvier, 1816

*Myliobatis* sp.

(Fig. 20)

**Referred specimens:** n = 30: ASIZF0100581–0100589, CMM F0378, F0379, F0381, F0383–F0387, F0389–F0393, F0394, F0396–F0398, F0410, F0411, F2855, NTM I01118.

**Description:** Each tooth of *Myliobatis* has a flat occlusal surface and is laterally elongated and hexagonal that may be straight or slightly arched. The root is polyaulocorhizous with well-defined anteroposteriorly oriented, vertical lamellar plates separated by deep grooves, where the crown overhangs the root on the labial (anterior) face. The lingual and labial faces are ornamented with a network of fine reticulated ridges that grade into longitudinal ridges in the apical and become finer and anastomotic.

**Remarks:** The tooth plates of *Myliobatis* are similar to those of *Aetomylaeus* and *Aetobatus*, but the lateral angle of the hexagonal tooth plates in *Aetomylaeus* is more oblique than that of *Myliobatis* (Ebersole, Cicimurri & Stringer, 2019). The vertical lamellar plates of the root in *Myliobatis* are coarser than *Aetobatus*. Teeth of *Myliobatis* lack the tuberculated enameloid on the occlusal surface, whereas teeth of *Aetomylaeus* are reticulated on the labial and lingual faces (Ebersole, Cicimurri & Stringer, 2019). Because the total morphological variation range of teeth in many of the aetobatid and myliobatid (Myliobatinae) species is unknown (e.g., see Hovestadt

& Hovestadt-Euler, 2013), we refrain from assigning the *Aetobatus* (see above) and *Myliobatis* teeth described here to the species level.

## Discussion

Published work on fossil elasmobranchs in Taiwan is very scarce, limited in scope, often lacked formal descriptions, and were mostly based on private collections (Lin et al., 2021). Huang (1965) reported three shark taxa while describing a fossil whale tympanic bone from the early Pleistocene Cholan Formation in northern Taiwan (as early Pliocene in Huang, 1965). Although the whereabouts of the specimens is unknown, it is one of the earliest accounts reporting fossil shark teeth in Taiwan. Uyeno (1978) listed nine elasmobranch taxa from the Pleistocene Chochen–Tsailiao area with images of the specimens but without descriptions. These specimens are reviewed in the present study.

Perhaps the most complete description on a single fossil shark assemblage in Taiwan is the one by Tao & Hu (2008) from the late Miocene **Tangenshan Sandstone Formation** in Chiahsien County, Kaohsiung. They described five taxa common in late Miocene marine deposits (*Otodus megalodon*, *Odontaspis* sp., †*Isurus hastalis*, †*Hemipristis serra*, and *Carcharhinus* sp.) as well as a new extinct species of *Hemipristis*, *H. liui* Tao & Hu, 2008. The specimen of *H. liui* is an upper tooth and is characterized by asymmetric serrations on the distal and mesial cutting edges. The occurrences of *Otodus megalodon* are sparsely recorded from Taiwan (Hu & Tao, 1993; Tao & Hu, 2008) and are mostly present in private collections, which is a potential direction for future research efforts (Haug et al., 2020; Lin et al., 2021).

The materials reviewed in this study were mainly based on surface collecting that spanned over three decades. We note that our bulk sediment sampling (830 kg, see methods) only yielded three specimens (ASIZF0100548, ASIZF0100590, and ASIZF0100591). Surface collecting likely results in sampling bias towards larger specimens, underrepresenting smaller specimens (Welton & Farish, 1993; Perez, 2022). Nevertheless, 697 elasmobranch teeth from the Liuchungchi Formation in Niubu described in this study document the presence of at least 20 elasmobranch taxa (Table 1). The excellent overall preservation allowed species-level taxonomic identification for most of the specimens, which in turn, permitted the elucidation of the diverse elasmobranch community. In fact, the assemblage represents the most diverse elasmobranch paleofaunas from Taiwan reported to date.

The species richness and diversity indices suggest that our assemblage is highly diverse even with respect to other contemporaneous assemblages from temperate and tropical West Pacific (Table 2). Importantly, the number of specimens reported from other assemblages is much lower compared to our material (Supplemental Table S1). However, the high species diversity in our collection likely reflects the geographic location of the study region, where both temperate and

tropical species overlap and accumulate. Similar condition is well recognized in marine fish fauna in Taiwan today (Ebert et al., 2013). Our present material indicates that this high diversity condition has preceded at least since the Pleistocene for the first time. Together, the high diversity captured in our study is significant in the spatio-temporal context.

The abundant and large teeth of *Carcharodon carcharias* are remarkable. *Carcharodon carcharias* is distributed along southern, eastern, and northeastern Taiwan today, but not on the west coast where the fossils are found (Teng, 1958; Shen, 1993; Ebert et al., 2013; Shao, 2022). According to the Fisheries Agency, Council of Agriculture, Taiwan (Taiwan Fisheries Agency, 2021), a total of 39 individuals of *C. carcharias* were caught between 2012 and 2021, with the majority of landings being in northeastern Taiwan. However, at our fossil sites, teeth of *C. carcharias* are the second most abundant fossils ( $n = 55$ ) identified to the species level in this study behind teeth of *Carcharhinus leucas* ( $n = 71$ , Table 1). Of the 55 isolated teeth that are interpreted to have most certainly come from 55 different individuals, 44 of them are well-preserved, allowing for tooth position identifications and accurate crown height measurements (CH). Based on the linear regression equation between the CH and total length (TL) for each tooth position in extant *Carcharodon carcharias* presented by Shimada (2003), the CH of each of the 44 teeth was used to estimate the TL of each fossil individual (Supplemental Table S2). Our specimens are normally distributed (Shapiro–Wilk test = 0.853,  $p = 0.08$ ) and range in TL from 1.9 to 5.6 m, with a mean of 3.5 m (Supplemental Table S2), suggesting the presence of many mature, large individuals (Ebert et al., 2013).

One of the most noteworthy occurrences reported in this study is that of the extinct species †*Hemipristis serra*. The species is known worldwide, but most of the documented occurrences are from the Miocene and Pliocene deposits (e.g., Yabumoto & Uyeno, 1994; Sánchez-Villagra et al., 2000; Marsili et al., 2007; Portell et al., 2008; Visaggi & Godfrey, 2010; Carrillo-Briceño et al., 2015; Kocsis et al., 2019). The fossil record indicates that the fossil species preferred warm neritic environments (Cappetta, 2004, 2012). Although most previous studies suggest its last appearance at the end of the Pliocene, new evidence indicates that †*H. serra* persisted into the Pleistocene in North America (Ebersole, Ebersole & Cicimurri, 2017; Boessenecker, Boessenecker & Geisler, 2018; Perez, 2022). Teeth of *Hemipristis* that may belong to *H. serra* have been reported from Pleistocene and ‘Plio-Pleistocene’ deposits in Sulawesi and Java, Indonesia (*H. cf. serra* by Hooijer, 1954, 1958; simply “*Hemipristis*” by Yudha et al., 2018). Previous records of †*H. serra* from Taiwan were reported by Uyeno (1978) from an uncertain stratigraphic horizon along Tsailiao River, and that by Tao & Hu (2008) from the Miocene Kueichulin Formation in southern Taiwan. The †*H. serra* specimens described here are the first confirmed Pleistocene record in Taiwan, and along with the putative Indonesian records (Hooijer, 1954, 1958; Yudha et al., 2018), the geologically youngest records of the extinct species in the Northwest Pacific, meaning that the North American occurrences were not isolated.

The assemblage described here is dominated by two genera, *Carcharhinus* (Carcharhinidae, n = 462) and *Carcharodon* (Lamnidae, n = 52), which comprise more than 77.5% of the total specimen count and about half of the taxa identified (11 out of 20). From a paleoecological perspective, the composition is roughly similar to that found in modern western Taiwan (Ebert et al., 2013; Shao, 2022). For example, the most abundant species of *Carcharhinus* in this study, *C. leucas*, presently lives in coastal areas of tropical and subtropical riverine and lacustrine environments (Compagno, 1984). The second-most abundant species in this study, *Carcharodon carcharias*, inhabits inshore shallow water to open ocean and, as a top predator, feeds on larger marine mammals and fishes (Ebert et al., 2013; Compagno, 2002). While pelagic sharks *Carcharhinus plumbeus* and *C. longimanus* are also represented in this Pleistocene assemblage, the occurrences of *C. altimus*, *Aetobatus* sp., and *Myliobatis* sp. may suggest the possible presence of deeper sandy, flat bottoms (Compagno, 1984). The abundant associated marine vertebrate fossils, including teleost bones (Tao, 1993), otoliths (Lin et al., 2018), and whale bones (Xue, 2004), indicate a rich, thriving marine ecosystem in the area. The sedimentary environment of the Liuchungchi Formation further points to shoreface to inner offshore setting, with several transgressive and regressive cycles (Chen, 2016). Taken together, the coastal areas in southwest Taiwan during the early Pleistocene can be interpreted as an inshore to offshore shallow-water environment with sandy bottoms.

## Conclusions

The fossil elasmobranch fauna from the tropical-subtropical West Pacific is poorly known compared to its modern analog, impeding our understanding of the formation of this current marine biodiversity hotspot. Using elasmobranch fossils from an early Pleistocene locality in southern Taiwan, we report a highly diverse shark and ray fauna from the region. The taxonomic composition of the assemblage reveals a nearshore shallow-water paleoenvironment which supports the sedimentary interpretation. In addition, the presence of †*Hemipristis serra* and large specimens of *Carcharodon carcharias* highlight the potential for studying fossils from underrepresented regions and stimulate similar studies from associated strata and localities. The present study can be regarded as the most extensive on elasmobranch fossils from Taiwan.

## Acknowledgements

We would like to express our sincere gratitude to Prof. Hsi-Jen Tao (National Taiwan University) who donated the specimens to the Biodiversity Research Museum, Academia Sinica, Taiwan. We also thank Mrs. Hsiao I-Ju (Chiayi Municipal Museum, CMM) for her administrative assistance in examining the CMM collection, and Miss Sun You-Yu (National Taiwan Museum) for accessing the collection described by Uyeno (1978). This manuscript has been improved based on constructive reviews by Kenneth De Baets, Dana Ehret, Laszlo Kocsis, and an anonymous reviewer.

# References

- Agassiz L. 1833–1843. *Recherches sur les poissons fossils: une introduction à l'étude de ces animaux*. Neuchatel, Switzerland: Imprimerie de Petitpierre.
- Agassiz L. 1858. A new species of skate from the Sandwich Islands. *Proceedings of the Boston Society of Natural History* 6 (1856–1859):385.
- Bellwood DR, Meyer CP. 2009. Searching for heat in a marine biodiversity hotspot. *Journal of Biogeography* 36:569–576 DOI: 10.1111/j.1365-2699.2008.02029.x.
- Berg LS. 1958. *System der rezenten und fossilen fischartigen und fische*. Berlin: Deutsche Verlag Wissenschaften.
- Blainville HMD de. 1816. Prodrome d'une nouvelle distribution systematique de regne animal. *Bulletin de Sciences de la Société Philomatique de Paris* 8:113–124.
- Bleeker P. 1852. Bijdrage tot de kennis der Plagiostomen van den Indischen Archipel. *Verhandelingen van het Bataviaasch Genootschap van Kunsten en Wetenschappen* 24:1–92.
- Bleeker P. 1854. Faunae ichthyologicae japonicae species novae. *Natuurkundig Tijdschrift voor Nederlandsch Indië* 6:395–426.
- Boessenecker SJ, Boessenecker RW, Geisler JH. 2018. Youngest record of the extinct walrus *Ontocetus emmonsii* from the Early Pleistocene of South Carolina and a review of North Atlantic walrus biochronology. *Acta Palaeontologica Polonica* 63:279–286 DOI: 10.4202/app.00454.2018.
- Bonaparte CL. 1835. Prodromus systematis ichthyologiae. *Nuovi Annali delle Scienze naturali Bologna (Ser. 1) (ann. 2)* 4:181–196, 272–277.
- Bonaparte CL. 1835. Prodromus systematis ichthyologiae. *Nuovi Annali delle Scienze naturali Bologna (Ser. 1) (ann. 2)* 4:181–196, 272–277.
- Bonaparte CL. 1840. *Iconografia della fauna italica per le quattro classi degli animali vertebrati. Tomo III*. Roma: Dalla Tipografia Salviucci.
- Buckeridge JS, Chan BKK, Lee S-W. 2018. Accumulations of fossils of the whale barnacle *Coronula bifida* Bronn, 1831 (Thoracica: coronulidae) provides evidence of a Late Pliocene cetacean migration route through the Straits of Taiwan. *Zoological Studies* 57:1–12.
- Cappetta H. 2004. *Handbook of Paleoichthyology, Vol. 3B: Chondrichthyes II Mesozoic and Cenozoic Elasmobranchii*. München: Verlag Dr Friedrich Pfeil.
- Cappetta H. 2012. *Handbook of Paleoichthyology, Vol. 3E: Chondrichthyes Mesozoic and Cenozoic Elasmobranchii: Teeth*. München: Verlag Dr Friedrich Pfeil.
- Carrillo-Briceño JD, De Gracia C, Pimiento C, Aguilera OA, Kindlimann R, Santamarina P, Jaramillo C. 2015. A new Late Miocene chondrichthyan assemblage from the Chagres Formation, Panama. *Journal of South American Earth Sciences* 60:56–70 DOI: 10.1016/j.jsames.2015.02.001
- Chen W-S. 2016. *An introduction to the geology of Taiwan*. Taipei: Geological Society of Taiwan.

- 757 Chen W-S, Huang N-E, Yang C-C. 2011. Pleistocene sequence stratigraphic characteristics and  
758 foreland basin evolution, southwestern Taiwan. *Special Publication of the Central*  
759 *Geological Survey* 25:1–38.
- 760 Chou J-T. 1975. A sedimentologic study of the Miocene Pachangchi Sandstone in the Chiayi  
761 region, Western Taiwan. *Petroleum Geology of Taiwan* 12:81–96.
- 762 Cigala-Fulgosi F, Mori D. 1979. Osservazioni tassonomiche sul genere Galeocerdo (Selachii,  
763 Carcharhinidae) con particolare riferimento a Galeocerdo cuvieri (Peron & Lesueur) nel  
764 Pliocene del Mediterraneo. *Bollettino della Societa Paleontologica Italiana* 18:117–132.
- 765 Compagno LJV. 1973. Interrelationships of living elasmobranchs. *Zoological Journal of the*  
766 *Linnean Society* 53:15–61.
- 767 Compagno LJV. 1984. *FAO species catalogue. Sharks of the world: An annotated and illustrated*  
768 *catalogue of shark species known to date, Volume 4: Carcharhiniformes*. Rome: Food and  
769 Agriculture Organization of the United Nations.
- 770 Compagno LJV. 1988. *Sharks of the order Carcharhiniformes*. New Jersey: Princeton University  
771 Press.
- 772 Compagno, LJV. 2002. *FAO species catalogue. Sharks of the world: An annotated and*  
773 *illustrated catalogue of shark species known to date, Volume 2: Bullhead, mackerel and*  
774 *carpet sharks (Heterodontiformes, Lamniformes and Orectolobiiformes)*. Rome: Food and  
775 Agriculture Organization of the United Nations.
- 776 Covey M. 1984. Lithofacies analysis and basin reconstruction, Plio-Pleistocene western Taiwan  
777 foredeep. *Petroleum Geology of Taiwan* 20:53–83.
- 778 Cuvier GLFCD. 1816. Le Règne Animal distribué d'après son organization, pour servir de base à  
779 l'histoire naturelle des animaux et d'introduction a l'anatomie comparée. *Les reptiles, les*  
780 *poissons, les mollusques et les annélides. Paris, 4 Vols, Edition 1. Poissons* 2:104–351.
- 781 Ebersole JA, Ebersole SM, Cicimurri DJ. 2017. The occurrence of early Pleistocene marine fish  
782 remains from the Gulf Coast of Mobile County, Alabama, USA. *Palaeodiversity*  
783 10:97–115 DOI: 10.18476/pale.v10.a6.
- 784 Ebersole JA, Cicimurri DJ, Stringer GL. 2019. Taxonomy and biostratigraphy of the  
785 elasmobranchs and bony fishes (Chondrichthyes and Osteichthyes) of the lower-to-middle  
786 Eocene (Ypresian to Bartonian) Claiborne Group in Alabama, USA, including an analysis  
787 of otoliths. *European Journal of Taxonomy* 585:1–274.
- 788 Ebert DA, White WT, Ho H-C, Last PR, Nakaya K, Séret B, Straube N, Naylor GJP, De  
789 Carvalho MR. 2013. An annotated checklist of the chondrichthyans of Taiwan. *Zootaxa*  
790 3752:279–386
- 791 Ebert DA, Dando M, Fowler S. 2021. *Shark of the world, A complete guide*. New Jersey:  
792 Princeton University Press.
- 793 Ehret DJ, MacFadden BJ, Jones DS, Devries TJ, Foster DA, Salas-Gismondi R. 2012.  
794 Origin of the white shark *Carcharodon* (Lamniformes: Lamnidae) based on  
795 recalibration of the Upper Neogene Pisco Formation of Peru. *Palaeontology* 55:1139–  
796 1153 DOI: 10.1111/j.1475-4983.2012.01201.x.



- 797 Fisher RA, Corbet AS, Williams CB. 1943. The relation between the number of species and the  
798 number of individuals in a random sample of an animal population. *The Journal of Animal*  
799 *Ecology* 12:42–58.
- 800 Fricke R, Eschmeyer WN, Van der Laan R, eds. 2022. Eschmeyer’s catalog of fishes: genera,  
801 species, references, version 02/2022, *Available at*  
802 <http://researcharchive.calacademy.org/research/ichthyology/catalog/fishcatmain.asp>  
803 (accessed May 2022).
- 804 Froese R, Pauly D, eds. 2022. FishBase. World Wide Web electronic publication.  
805 [www.fishbase.org](http://www.fishbase.org), version 02/2022, *Available at* <https://www.fishbase.se/search.php>  
806 (accessed July 2022).
- 807 Garrick JAF. 1982. Sharks of the genus *Carcharhinus*. NOAA Technical Report NMFS Circular  
808 445, Seattle, Washington: NMFS Scientific Publications Office.
- 809 Griffith E, Smith CH. 1834. The class Pisces, arranged by the Baron Cuvier, with supplementary  
810 additions, by Edward Griffith, F.R.S., &c. and Lieut.-Col. Charles Hamilton Smith, C. H.,  
811 K. W., F. R., L. S. S., &c. &c. In: Cuvier G, ed. *The animal kingdom arranged in*  
812 *conformity with its organization, with additional descriptions of all the species hitherto*  
813 *named, and of many not before noticed, by Edward Griffith, and others*. London: Whittaker  
814 & Co.
- 815 Hasse JCF. 1878. Das natürliche System des Elasmobranchier auf Grundlage des Baues und der  
816 Entwicklung des Wirbelsäule. *Zoologischer Anzeiger* 1:144–148, 167–172, 7:144–148,  
817 8:167–172.
- 818 Haug C, Reumer JWF, Haug JT, et al. 2020. Comment on the letter of the Society of Vertebrate  
819 Paleontology (SVP) dated April 21, 2020 regarding “Fossils from conflict zones and  
820 reproducibility of fossil-based scientific data”: the importance of private collections.  
821 *Paläontologische Zeitschrift* 94:413–429 DOI: 10.1007/s12542-020-00522-x.
- 822 Herman J, Hovestadt-Euler M, Hovestadt DC. 1998. Contributions to the study of the  
823 comparative morphology of teeth and other relevant ichthyodorulites in living  
824 supraspecific taxa of Chondrichthyan fishes. Part B: Batomorphii 4a: Order Rajiformes –  
825 Suborder Myliobatoidei – Superfamily Dasyatoidea – Family Dasyatidae – Subfamily  
826 Dasyatinae – Genera: *Amphotistius*, *Dasyatis*, *Himantura*, *Pastinachus*, *Pteroplatytrygon*,  
827 *Taeniura*, *Urogymnus* and *Urolophoides* (incl. supraspecific taxa of uncertain status and  
828 validity), Superfamily Myliobatoidea – Family Gymnuridae – Genera: *Aetoplatea* and  
829 *Gymnura*, Superfamily Plesiobatoidea – Family Hexatrygonidae – Genus: *Hexatrygon*.  
830 *Bulletin de l'Institut Royal des Sciences Naturelles de Belgique, Biologie* 68:145–197.
- 831 Herman J, Hovestadt-Euler M, Hovestadt DC. 1999. Contributions to the study of the  
832 comparative morphology of teeth and other relevant ichthyodorulites in living  
833 supraspecific taxa of Chondrichthyan fishes. Part B: Batomorphii 4b: Order Rajiformes –  
834 Suborder Myliobatoidei – Superfamily Dasyatoidea – Family Dasyatidae – Subfamily  
835 Dasyatinae – Genera: *Taeniura*, *Urogymnus*, *Urolophoides* – Subfamily  
836 Potamotrygoninae – Genera: *Disceus*, *Plesioptrygon*, and *Potamotrygon* (incl. supraspecific  
837 taxa of uncertain status and validity), Family Urolophidae – Genera: *Trygonoptem*,  
838 *Urolophus* and *Urotrygon* – Superfamily Myliobatoidea – Family Gymnuridae – Genus:  
839 *Aetoplatea*. *Bulletin de l'Institut Royal des Sciences Naturelles de Belgique, Biologie*

- 840 69:161–200.
- 841 Herman J, Hovestadt-Euler M, Hovestadt DC. 2000. Contributions to the study of the  
842 comparative morphology of teeth and other relevant ichthyodorulites in living  
843 supraspecific taxa of Chondrichthyan fishes. Part B: Batomorphii 4c: Order Rajiformes –  
844 Suborder Myliobatoidei – Superfamily Dasyatoidea – Family Dasyatidae – Subfamily  
845 Dasyatinae – Genus: *Urobatis*, Subfamily Potamotrygoninae – Genus: *Paratrygon*,  
846 Superfamily Plesiobatoidea – Family Plesiobatidae – Genus: *Plesiobatis*, Superfamily  
847 Myliobatoidea – Family Myliobatidae - Subfamily Myliobatinae – Genera : *Aetobatus*,  
848 *Aetomylaeus*, *Myliobatis* and *Pteromylaeus*, Subfamily Rhinopterinae – Genus: *Rhinoptera*  
849 and Subfamily Mobulinae – Genera: *Manta* and *Mobula*. Addendum 1 to 4a: erratum to  
850 Genus *Pteroplatytrygon*. *Bulletin de l'Institut Royal des Sciences Naturelles de Belgique*,  
851 *Biologie* 70:5–67.
- 852 Ho C-S. 1967. Foothill tectonics of Taiwan. *Bulletin of the Geological Survey of Taiwan* 25:9–  
853 28.
- 854 Ho C-S. 1976. Structural evolution of Taiwan, *Tectonophysics* 4:367–378.
- 855 Hooijer D. 1954. Pleistocene vertebrates from Celebes. IX. Elasmobranchii. X. Testudinata.  
856 *Proceedings of the Koninklijke Nederlandse Akademie van Wetenschappen, Series B*,  
857 57:475–789.
- 858 Hooijer DA. 1958. The Pleistocene vertebrate fauna of Celebes. *Asian Perspectives* 2(2):71-76.
- 859 Hovestadt DC, Hovestadt-Euler M. 2013. Generic assessment and reallocation of Cenozoic  
860 Myliobatinae based on new information of tooth, tooth plate and caudal spine morphology  
861 of extant taxa. *Palaeontos* 24:1–66.
- 862 Hu C-H. 1989. Manual for ten geological routes in central Taiwan—route 7: geology along the  
863 Nanheng Highway—Tsailiao, Peiliao, Chiahhsien. In: Faculty members of the Department  
864 of Earth Sciences, National Taiwan Normal University, editors. *Field manual of the*  
865 *geology of Taiwan (II)*. Taipei: Department of Earth Sciences, National Taiwan Normal  
866 University, 105–163.
- 867 Hu C-H, Tao H-J. 1993. *The fossil faunas of Penghu Islands, Taiwan*. Penghu: Penghu District  
868 Cultural Center Publications.
- 869 Hu C-H, Tao H-J. 1996. *Crustacean fossils of Taiwan*. Taipei: San Min Book.
- 870 Hu C-H, Tao H-J. 2004. Studies on the Neogene crabs from south-western foothills of Taiwan.  
871 *Acta Palaeontologica Sinica* 43(4):537–555.
- 872 Huang T. 1965. A new species of a whale tympanic bone from Taiwan, China. *Transaction and*  
873 *Proceedings of the Palaeontological Society of Japan* 61:183–187.
- 874 Huang W-C. 2010. Stratigraphic sequences in distal part of foreland Basin in Southwestern  
875 Taiwan: Model of interplay between tectonics and eustasy. Master Thesis, Department of  
876 Earth Sciences, National Cheng Kung University.
- 877 Hubbell G. 1996. *Using tooth structure to determine the evolutionary history of the white shark.*  
878 *In Great white sharks: the biology of Carcharodon Carcharias*. San Diego: Academic  
879 Press.

- 880 Huxley TH. 1880. On the application of the laws of evolution to the arrangement of the  
881 Vertebrata, and more particularly of the Mammalia. *Proceedings of the Zoological Society*  
882 *of London* 43:649–662.
- 883 Jordan DS, Gilbert CH. 1879. Notes on the fishes of Beaufort Harbor, North Carolina.  
884 *Proceedings of the United States National Museum* 55:365–388.
- 885 Jordan DS, Evermann BW. 1896. The fishes of North and Middle America. *Bulletin of the*  
886 *United States National Museum* 47:1–1240.
- 887 Kajiura SM, Tricas T. 1996. Seasonal dynamics of dental dimorphism in the Atlantic Stingray  
888 *Dasyatis sabina*. *Journal of Experimental Biology* 199:2297–306.
- 889 Karasawa H. 1989. Late Cenozoic elasmobranchs from the Hokuriku district, central Japan. *The*  
890 *science reports of the Kanazawa University* 34(1):1–57.
- 891 Kawase M, Nishimatsu K. 2016. Elasmobranch remains from the Middle Pleistocene Takamatsu  
892 Silty Sandstone of the Toyohashi Formation, the Atsumi Group, Aichi Prefecture, Central  
893 Japan. *Bulletin of the Mizunami Fossil Museum* 42:47–61.
- 894 Kocsis L, Botfalvai G, Qamarina Q, Razak H, Király E, Lugli F, Wings O, Lambertz M, Raven  
895 H, Briguglio A, Rabi M. 2021. Geochemical analyses suggest stratigraphic origin and late  
896 Miocene age of reworked vertebrate remains from Penanjong Beach in Brunei Darussalam  
897 (Borneo). *Historical Biology* 33(11):2627–2638.
- 898 Kocsis L, Briguglio A, Cipriani A, Frijia G, Vennemann T, Baumgartner C, Roslim A. 2022.  
899 Strontium isotope stratigraphy of late Cenozoic fossiliferous marine deposits in North  
900 Borneo (Brunei, and Sarawak, Malaysia). *Journal of Asian Earth Sciences* DOI:  
901 10.1016/j.jseas.2022.105213.
- 902 Kocsis L, Razak H, Briguglio A, Szabó M. 2019. First report on a diverse Neogene fossil  
903 cartilaginous fish fauna from Borneo (Ambug Hill, Brunei Darussalam). *Journal of*  
904 *Systematic Palaeontology* 17(10):791–819 DOI:  
905 10.1080/14772019.2018.1468830.
- 906 Koumans FP. 1949. On some fossil fish remains from  
907 Java. *Zoologische Mededelingen* 30(5):77–82.
- 908 Last, PR, Naylor GJP, Manjaji-Matsumoto BM. 2016. A revised classification of the family  
909 Dasyatidae (Chondrichthyes: Myliobatiformes) based on new morphological and  
910 molecular insights. *Zootaxa* 4139:345–368.
- 911 Lesueur CA. 1818. Description of several new species of North American fishes. *Journal of the*  
912 *Philadelphia Academy of Natural Sciences* 1:222–235.
- 913 Lin A-T, Watts AB. 2002. Origin of the west Taiwan basin by orogenic loading and flexure of a  
914 rifted continental margin. *Journal of Geophysical Research* 107:2185.
- 915 Lin C-H, Chien C-W. 2022. Late Miocene otoliths from northern Taiwan: insights into the rarely  
916 known Neogene coastal fish community of the subtropical northwest Pacific. *Historical*  
917 *Biology* 34:361–382 DOI: 10.1080/08912963.2021.1916012
- 918 Lin C-H, Chien C-W, Lee S-W, Chang C-W. 2021. Fossil fishes of Taiwan, a review and  
919 prospection. *Historical Biology* 33:1362–1372 DOI: 10.1080/08912963.2019.1698563.
- 919 Lin C-H, Ou H-Y, Lin C-Y, Chen H-M. 2022. First skeletal fossil record of the red

- 920 seabream *Pagrus major* (Sparidae, Perciformes) from the Late Pleistocene of subtropical  
921 West Pacific, southern Taiwan. *Zoological Studies* 61:10 DOI: 10.6620/ZS.2022.61-10.
- 922 Lin C-H, Wang L-C, Wang C-H, Chang C-W. 2018. Common early Pleistocene fish otoliths  
923 from Niubu in Chia-Yi County, southwestern Taiwan. *Journal of the National Taiwan*  
924 *Museum* 71:47–68 DOI: 10.6532/JNTM.201809\_71(3).04.
- 925 Linnaeus C. 1758. *Systema naturae per regna tria naturae, secundum classes, ordines, genera,*  
926 *species, cum characteribus, differentiis, synonymis, locis, vol. I.* Stockholm: Laurentii  
927 Salvii.
- 928 Lundberg N, Reed DL, Liu C-S, Lieske J. 1997. Forearc-basin closure and arc accretion in the  
929 submarine suture zone south of Taiwan. *Tectonophysics* 274:5–23.
- 930 Marsili S, 2006. Revision of the teeth of the genus *Carcharhinus* (Elasmobranchii;  
931 *Carcharhinidae*) from the Pliocene of Tuscany, Italy. *Rivista Italiana di Paleontologia e*  
932 *Stratigrafia* 113:79–95 DOI: 10.13130/2039-4942/6360.
- 933 Marsili S, Carnevale G, Danese E, Bianucci G, Landini W. 2007. Early Miocene vertebrates  
934 from Montagna della Maiella, Italy. *Annales de Paléontologie* 93:1, 27–66 DOI:  
935 10.1016/j.annpal.2007.01.001.
- 936 Müller J, Henle FGJ. 1837. *Gattungen der Haifische und Rochen nach einer vom ihm mit Hr*  
937 *Henle unternommenen gemeinschaftlichen Arbeit über die Naturgeschichte der*  
938 *Knorpelfische*. Berlin: Berichte der königlich preussischen Akademie der Wissenschaften.
- 939 Müller J. Henle FGJ. 1838. On the generic characters of cartilaginous fishes. *Magazine of*  
940 *Natural History* 2:33–91.
- 941 Müller J, Henle J. 1839. *Systematische Beschreibung der Plagiostomen*. Berlin: Verlag von veit  
942 und comp.
- 943 Myers N, Mittermeier RA, Mittermeier CG, da Fonseca GAB, Kent J. 2000. Biodiversity  
944 hotspots for conservation priorities. *Nature* 403:853–858.
- 945 Nagel S, Castelltort S, Wetzel A, Willett SD, Mouthereau F, Lin A-T. 2013. Sedimentology and  
946 foreland basin paleogeography during Taiwan arc continent collision. *Journal of Asian*  
947 *Earth Sciences* 62:180–204.
- 948 Nardo GD. 1827. Prodromus observationum et disquisitionum Adriaticae ichthyologiae.  
949 *Giornale di fisica, chimica e storia naturale, ed arti* 10:22–40.
- 950 Naylor GJP, Marcus LF. 1994. Identifying isolated shark teeth of the genus *Carcharhinus* to  
951 species relevance for tracking phyletic change through the fossil record. *American Museum*  
952 *Novitates* 3109:56.
- 953 Nelson JS, Grande TC, Wilson MVH. 2016. *Fishes of the world*. New Jersey: John Wiley &  
954 Sons.Perez VJ. 2022. The chondrichthyan fossil record of the Florida Platform  
955 (Eocene–Pleistocene). *Paleobiology*, 1–33 DOI: 10.1017/pab.2021.47.
- 956 Péron F, Lesueur CA. 1822. Description of a *Squalus*, of a very large size, which was taken  
957 on the coast of New Jersey. *Journal of the Philadelphia Academy of Natural Sciences*  
958 2:343–352.
- 959 Poey F. 1861. Conspectus piscium cubensium. In: *Memorias sobre la historia natural de la*

- 960 *Isla de Cuba, acompañadas de sumarios Latinos y extractos en Francés*. Barcina, La  
961 Habana: ealle de la Reina, 337–442.
- 962 Portell RW, Hubbell G, Donovan SK, Green JL, Harper DAT, Pickerill R. 2008. Miocene  
963 sharks in the Kendeace and Grand Bay formations of Carriacou, The Grenadines,  
964 Lesser Antilles. *Caribbean Journal of Science* 44:279–286 DOI:  
965 10.18475/cjos.v44i3.a2.
- 966 Purdy RW, Schneider VP, Applegate SP, McLellan JH, Meyer RL, Slaughter BH. 2001. The  
967 Neogene sharks, rays, and bony fishes from Lee Creek Mine, Aurora, North Carolina.  
968 In Ray CE, Bohaska DH, eds. *Geology and Paleontology of the Lee Creek Mine,*  
969 *North Carolina, III: Smithsonian Contributions to Paleobiology*. Washington:  
970 Smithsonian Institution Press, 71–160.
- 971 Purdy RW. 2006. A key to common genera of Neogene shark teeth. *Available at*  
972 <http://paleobiology.si.edu/pdfs/sharktoothKey.pdf> (accessed May 2022).
- 973 Rafinesque CS. 1810. *Caratteri di alcuni nuovi generi e nuove specie di animali e piante*  
974 *della Sicilia, con varie osservazioni sopra i medesimi*. Palermo, Italy: Sanfilippo.
- 975 Ribas-Deulofeu L, Wang Y-C, Lin C-H. 2021. First record of Late Miocene *Dendrophyllia*  
976 *de Blainville, 1830 (Scleractinia: Dendrophylliidae)* in Taiwan. *Terrestrial,*  
977 *Atmospheric and Oceanic Sciences* 32:1061–1068 DOI: 10.3319/TAO.2021.09.13.02.
- 978 Rüppell WPES. 1837. *Neue Wirbelthiere zu der Fauna von Abyssinien gehörig entdeckt und*  
979 *beschrieben von Dr. Eduard Ruppell*. Frankfurt am Main: Fische des Rothen Meeres,  
980 Siegmund Schmerber.
- 981 Sánchez-Villagra MR, Burnham RJ, Campbell DC, Feldmann RM, Gaffney ES, Kay RF,  
982 Lozsan R, Purdy R, Thewissen JGM. 2000. A new near-shore marine fauna and flora  
983 from the Early Neogene of northwestern Venezuela. *Journal of Paleontology* 74:957–  
984 968 DOI:10.1017/s0022336000033126.
- 985 Shannon CE. 1948. A mathematical theory of communication. *The Bell System Technical*  
986 *Journal* 27(3):379–423.
- 987 Shao K-T. 2022. Taiwan Fish Database. WWW Web electronic publication. *Available at*  
988 <http://fishdb.sinica.edu.tw> (accessed July 2022).
- 989 Shen S-C. 1993. *Fishes of Taiwan*. Taipei: Department of Zoology, National Taiwan  
990 University.
- 991 Shimada K. 2002. Dental homologies in lamniform sharks (Chondrichthyes: Elasmobranchii).  
992 *Journal of Morphology* 251:38–72.
- 993 Shimada K. 2003 (date of imprint 2002). The relationship between the tooth size and total body  
994 length in the white shark, *Carcharodon carcharias*. *Journal of Fossil Research* 35:28–33.
- 995 Simpson EH. 1949. Measurement of diversity. *Nature* 163:688.
- 996 Smith A. 1938. In: Müller J, Henle FGJ, eds. On the generic characters of cartilaginous fishes,  
997 with descriptions of new genera. *Magazine of Natural History* 2:33–37, 88–91.

- 998 Smith JLB. 1957. The rare shark *Hemipristis elongatus* (Klunzinger), 1871, from Zanzibar and  
999 Mozambique. *Annals and Magazine of Natural History* 10:555–560 DOI:  
1000 10.1080/00222935708655997.
- 1001 Springer S. 1950. A revision of North American sharks allied to the Genus *Carcharhinus*.  
1002 *American Museum Novitates* 1451:1–13.
- 1003 Stach LW. 1957. Stratigraphic subdivision and correlation of the upper Cenozoic sequence in the  
1004 foothills region east of Chiayi and Hsinying, Taiwan, China. *Symposium on Petroleum*  
1005 *Geology of Taiwan*, 177–230.
- 1006 Suppe J. 1984. Kinematics of arc-continent collision, flipping of subduction, and back-arc  
1007 spreading near Taiwan. *Journal of the Geological Society of China* 6:21–33.
- 1008 Taiwan Fisheries Agency. 2021. Coastal great white sharks, megamouth sharks, elephant sharks,  
1009 manta rays reported statistics. Fisheries Agency, Taipei, Taiwan.
- 1010 Tanaka T, Taru H. 2022. Fossil elasmobranchs from the Iimuro Formation, Kazusa Group,  
1011 Lower Pleistocene, Komae City, Tokyo, Japan. *Natural History Report of Kanagawa*  
1012 43:147–156 DOI: 10.32225/nkpmnh.2022.43\_147.
- 1013 Taniuchi T, Shimizu M. 1993. Dental sexual dimorphism and food habits in the stingray  
1014 *Dasyatis akajei* from Tokyo Bay, Japan. *Nippon Suisan Gakkaishi* 59:53–60.
- 1015 Tao H-J. 1993. A new Miocene fossil species *Priacanthus liui* (Pisces: perciformes) from the  
1016 Nanchung Formation in Chiayi Hsien, Taiwan. *Bulletin of the National Museum of Nature*  
1017 *and Science* 4:91–100.
- 1018 Tao H-J, Hu C-H. 2008. Fossil chondrichthyes fishes of Chia-hsien, Kaoshung County, Taiwan.  
1019 *Journal of the National Taiwan Museum* 61:41–62.
- 1020 Teng H-T. 1958. Studies on the elasmobranch fishes from Formosa. Part 1. Eighteen unrecorded  
1021 species of sharks from Formosa. *Reports of the Laboratory of Fishery Biology, Taiwan*  
1022 *Fisheries Research Institute* 3:1–30.
- 1023 Teng L-S. 1990. Geotectonic evolution of late Cenozoic arc-continent collision in Taiwan.  
1024 *Tectonophysics* 183:57–76.
- 1025 Türtscher J, López-Romero FA, Jambura PL, Kindlimann R, Ward DJ, Kriwet J. 2021.  
1026 Evolution, diversity, and disparity of the tiger shark lineage *Galeocerdo* in deep time.  
1027 *Paleobiology* 47:574–590 DOI: 10.1017/pab.2021.6.
- 1028 Uyeno T. 1978. A preliminary report on fossil fishes from Ts’o-chen Tainan. *Science Report*  
1029 *Geology and Paleontology* 1:5–17.
- 1030 Valenciennes A. 1839. In: Müller J, Henle FGJ, eds. *Systematische Beschreibung der*  
1031 *Plagiostomen*, vol. 2. Berlin: Verlag von veit und comp, 39–102.
- 1032 Visaggi CC, Godfrey SJ. 2010. Variation in composition and abundance of Miocene shark teeth  
1033 from Calvert Cliffs, Maryland. *Journal of Vertebrate Paleontology* 30:26–35 DOI:  
1034 10.1080/02724630903409063.
- 1035 Voigt M, Weber D. 2011. *Field guide for sharks of the genus Carcharhinus*. München:  
1036 Verlag Dr. Friedrich Pfeil.

- Weigmann S. 2016. Annotated checklist of the living sharks, batoids and chimaeras (Chondrichthyes) of the world, with a focus on biogeographical diversity. *Journal of Fish Biology* 88:837–1037 DOI: 10.1111/jfb.12874.
- Welton BJ, Farish RF. 1993. *The collector's guide to Fossil Sharks and Rays from the Cretaceous of Texas*. Lewisville, Texas: Before Time.
- White WT. 2012. A redescription of *Carcharhinus dussumieri* and *C. sealei*, with resurrection of *C. coatesi* and *C. tjutjot* as valid species (Chondrichthyes: Carcharhinidae). *Zootaxa* 3241:1–34.
- White WT, Kawauchi J, Corrigan S, Naylor G. 2015. Redescription of the eagle rays *Myliobatis hamlyni* Ogilby, 1911 and *M. tobijei* Bleeker, 1854 (Myliobatiformes: Myliobatidae) from the East Indo-West Pacific. *Zootaxa* 3948(3):521–548 DOI: 10.11646/zootaxa.3948.3.7.
- Whitenack LB, Gottfried MD. 2010. A morphometric approach for addressing tooth-based species delimitation in fossil mako sharks, *Isurus* (Elasmobranchii: Lamniformes). *Journal of Vertebrate Paleontology* 30:17–25 DOI: 10.1080/02724630903409055.
- Whitley GP. 1929. Studies in ichthyology. *Records of the Australian Museum* 17:101–143.
- Wilmers J, Waldron M, Bargmann S. 2021. Hierarchical microstructure of tooth enameloid in two Lamniform shark species, *Carcharias taurus* and *Isurus oxyrinchus*. *Nanomaterials* 11:969 DOI: 10.3390/nano11040969.
- Xue W-J. 2004. *Chiayi area fossil map*. Chiayi: Chiayi City Cultural Bureau.
- Yabumoto Y, Uyeno T. 1994. Late Mesozoic and Cenozoic fish faunas of Japan. *Island Arc* 3:255–269 DOI: 10.1111/j.1440-1738.1994.tb00115.x.
- Yu H-S, Chou Y-W. 2001. Characteristics and development of the flexural forebulge and basal unconformity of Western Taiwan Foreland Basin. *Tectonophysics* 333:277–291.
- Yudha DS, Ramadhani R, Suriyanto RA, Novian MI. 2018. The diversity of sharks fossils in Plio-Pleistocene of Java, Indonesia. *AIP Conference Proceedings* 2002(1):020013 DOI: 10.1063/1.5050109.

## Supplemental file

- Supplemental Figure S1. Aerial photographs of the Niubu locality showing the closest sampling site to the weir (red square, Site 1 in Fig. 2B). A, general view; B, C, closer views of the sampling site. Note the sandstones in the river bed transported from the upstream older strata.
- Supplemental Table S1. List of taxa and their abundance extracted from the Pleistocene elasmobranch assemblages from the West Pacific. Only teeth are included, i.e., spines, vertebrae and other remains are not included. Nomenclatures remain as those reported in the literature.
- Supplemental Table S2. Measurement, tooth position, and estimated fish total length of 44 better-preserved specimens of *Carcharodon carcharias* specimens from the early Pleistocene of Liuchungchi Formation of Niubu, southern Taiwan. \* = estimated crown height values for specimens with slightly worn apex.

# Figure captions

Figure 1. Summary of the sampling sites. A, overview of geological map of Taiwan (modified after Chen, 2016). B, geological map of Niubu area, Chiayi (map extracted from National Geological Data Warehouse, Central Geological Survey, MOEA). Yellow stars = sampling sites (see Fig. 2B for details). C, stratigraphic correlation of the Western Foothills (modified after Chen, 2016). Liuchungchi Formation is indicated in yellow.

Figure 2. A, stratigraphic column (modified after Huang, 2010). B, details of the sampling sites. GPS coordinates: Site 1 = 23°26'23.4"N, 120°35'35.5"E; Site 2 = 23°26'22.6"N, 120°35'32.7"E; Site 3 = 23°26'23.5"N, 120°35'29.8"E.

Figure 3. Teeth of *Carcharias taurus* from the early Pleistocene, Liuchungchi Formation of Niubu, southern Taiwan. A, B, ASIZF0100320; C–E, CMM F0204. A, C = lingual views; B, D = labial views; E = lateral view. Scale bar = 1 cm.

Figure 4. Teeth of *Carcharodon carcharias* from the early Pleistocene, Liuchungchi Formation of Niubu, southern Taiwan. A, B, ASIZF0100344; C, D, ASIZF0100337; E, F, ASIZF0100338; G, H, ASIZF0100336; I, J, ASIZF0100335; K, L, ASIZF0100339; M, N, ASIZF0100340; O, P, ASIZF0100324; Q, R, ASIZF0100328; S, T, ASIZF0100325; U, V, ASIZF0100326; W, X, ASIZF0100323. A, C, E, G, I, K, M, O, Q, S, U, W = lingual views; B, D, F, H, J, L, N, P, R, T, V, X = labial views. Scale bar = 1 cm.

Figure 5. Teeth of *Isurus oxyrinchus* from the early Pleistocene, Liuchungchi Formation of Niubu, southern Taiwan. A–C, ASIZF0100317; D–F, ASIZF0100318; G, H, ASIZF0100321; I, J, CMM F0242. A, D, G, I = lingual views; B, E, H, J = labial views; C, F = lateral views. Scale bar = 1 cm.

Figure 6. Teeth of †*Hemipristis serra* from the early Pleistocene, Liuchungchi Formation of Niubu, southern Taiwan. A, B, CMM F0232; C, D, ASIZF0100460; E, F, ASIZF0100461; G, H, ASIZF0100462. A, C, E, G = lingual views; B, D, F, H = labial views. Scale bars = 1 cm.

Figure 7. Teeth of *Carcharhinus altimus* from the early Pleistocene, Liuchungchi Formation of Niubu, southern Taiwan. A, B, ASIZF0100357; C, D, ASIZF0100359; E, F, CMM F0363; G, H, CMM F0293; I, J, CMM F0322; K, L, ASIZF 0100365. A, C, E, G, I, K = lingual views; B, D, F, H, J, L = labial views. Scale bar = 1 cm.

Figure 8. Teeth of *Carcharhinus amboinensis* from the early Pleistocene, Liuchungchi Formation of Niubu, southern Taiwan. A, B, CMM F0209; C, D, ASIZF0100368; E, F, ASIZF0100366; G,



1115 H, ASIZF0100369. A, C, E, G = lingual views; B, D, F, H = labial views. Scale bar = 1 cm.

1116

1117 Figure 9. Teeth of *Carcharhinus leucas* from the early Pleistocene, Liuchungchi Formation of  
1118 Niubu, southern Taiwan. A, B, ASIZF0100398; C, D, ASIZF0100397; E, F, ASIZF0100394; G,  
1119 H, ASIZF0100411; I, J, ASIZF0100396; K, L, ASIZF 0100395; M, N, ASIZF0100400; O, P,  
1120 ASIZF0100402; Q, R, ASIZF0100390. A, C, E, G, I, K, M, O, Q = lingual views; B, D, F, H, J,  
1121 L, N, P, R = labial views. Scale bar = 1 cm.

1122

1123 Figure 10. Teeth of *Carcharhinus limbatus* from the early Pleistocene, Liuchungchi Formation of  
1124 Niubu, southern Taiwan. A, B, ASIZF0100470; C, D, ASIZF0100476; E, F, ASIZF0100469; G,  
1125 H, ASIZF0100468; I, J, CMM F0236; K, L, CMM F0111; M, N, CMM F0237; O, P, CMM  
1126 F0238. A, C, E, G, I, K, M, O = lingual views; B, D, F, H, J, L, N, P = labial views. Scale bar = 1  
1127 cm.

1128

1129 Figure 11. Teeth of *Carcharhinus longimanus* from the early Pleistocene, Liuchungchi  
1130 Formation of Niubu, southern Taiwan. A, B, ASIZF 0100371; C, D, ASIZF0100376; E, F,  
1131 ASIZF0100370; G, H, ASIZF0100377; I, J, ASIZF0100375; K, L, ASIZF0100378; M, N,  
1132 ASIZF0100374; O, P, ASIZF0100373; Q, R, ASIZF0100392; S, T, ASIZF0100391. A, C, E, G,  
1133 I, K, M, O, Q, S = lingual views; B, D, F, H, J, L, N, P, R, T = labial views. Scale bar = 1 cm.

1134

1135 Figure 12. Teeth of *Carcharhinus obscurus* from the early Pleistocene, Liuchungchi Formation  
1136 of Niubu, southern Taiwan. A, B, ASIZF0100372; C, D, ASIZF0100384; E, F, ASIZF0100385;  
1137 G, H, ASIZF0100386; I, J, ASIZF0100388; K, L, ASIZF0100387; M, N, ASIZF0100383. A, C,  
1138 E, G, I, K, M = lingual views; B, D, F, H, J, L, N = labial views. Scale bar = 1 cm.

1139

1140 Figure 13. Teeth of *Carcharhinus plumbeus* from the early Pleistocene, Liuchungchi Formation  
1141 of Niubu, southern Taiwan. A, B, ASIZF0100412; C, D, ASIZF0100406; E, F, ASIZF0100405;  
1142 G, H, ASIZF0100410; I, J, ASIZF0100409; K, L, ASIZF0100408; M, N, ASIZF0100407. A, C,  
1143 E, G, I, K, M = lingual views; B, D, F, H, J, L, N = labial views. Scale bar = 1 cm.

1144

1145 Figure 14. Teeth of *Carcharhinus sorrah* from the early Pleistocene, Liuchungchi Formation of  
1146 Niubu, southern Taiwan. A, B, CMM F0129; C, D, CMM F0119; E, F, ASIZF0100418; G, H,  
1147 CMM F0126; I, J, CMM F0135; K, L, CMM F0122; M, N, CMM F0140. A, C, E, G, I, K, M =  
1148 lingual views; B, D, F, H, J, L, N = labial views. Scale bar = 1 cm.

1149

1150 Figure 15. Teeth of *Carcharhinus tjtjt* from the early Pleistocene, Liuchungchi Formation of  
1151 Niubu, southern Taiwan. A, B, ASIZF0100415; C, D, ASIZF0100414; E, F, CMM F0116; G, H,  
1152 ASIZF0100413; I, J, ASIZF0100417; K, L, ASIZF0100416; M, N, CMM F0323; O, P, CMM  
1153 F0324. A, C, E, G, I, K, M, O = lingual views; B, D, F, H, J, L, N, P = labial views. Scale bar = 1  
1154 cm.

1155

1156 Figure 16. Teeth of *Rhizoprionodon acutus* from the early Pleistocene, Liuchungchi Formation  
1157 of Niubu, southern Taiwan. A, B, ASIZF0100463; C, D, CMM F0120; E, F, CMM F0121; G, H,  
1158 CMM F0131; I, J, ASIZF0100464. A, C, E, G, I = lingual views; B, D, F, H, J = labial views.  
1159 Scale bar = 1 cm.

1160

1161 Figure 17. Teeth of *Galeocерdo cuvier* and *Sphyrna lewini* from the early Pleistocene,  
1162 Liuchungchi Formation of Niubu, southern Taiwan. A–H, *Galeocерdo cuvier*; A, B, CMM  
1163 F0245; C–E, CMM F0215; F–H, ASIZF0100459. I–L, *Sphyrna lewini*; I, J, CMM F0235; K, L,  
1164 CMM F0312. A, C, F, I, K = lingual views; B, D, G, J, L = labial views; E, H = details of  
1165 secondary serrations. Scale bars = 1 cm.

1166

1167 Figure 18. Teeth of *Dasyatidae* indet. from the early Pleistocene, Liuchungchi Formation of  
1168 Niubu, southern Taiwan. A–D, ASIZF0100590; E–H, ASIZF0100591. A, E = labial views; B, F  
1169 = basal views; C, G = occlusal views; D, H = lateral views. Scale bar = 5 mm.

1170

1171 Figure 19. Teeth of *Aetobatus* sp. from the early Pleistocene, Liuchungchi Formation of Niubu,  
1172 southern Taiwan. A, B, CMM F2854; C, D, CMM F2850; E, F, CMM F0408; G, H,  
1173 ASIZF0100549. A, C, E, G = occlusal views; B, D, F, H = basal views. Scale bar = 1 cm.

1174

1175 Figure 20. Teeth of *Myliobatis* sp. from the early Pleistocene, Liuchungchi Formation of Niubu,  
1176 southern Taiwan. A–D, ASIZF0100582; E–H, ASIZF0100587; I–L, ASIZF0100586; M, N,  
1177 CMM F0395; O, P, CMM F2855; Q, R, CMM F0393; S, T, CMM F0398. A, E, I, M, O, Q, S =  
1178 occlusal views; B, F, J, N, P, R, T = basal views; C, G, K = lingual views; D, H, L = labial  
1179 views. Scale bars = 1 cm.

1180

1181

## 1182 Table captions

1183 Table 1. Elasmobranchs from the early Pleistocene Liuchungchi Formation of Niubu, southern  
1184 Taiwan.

1185 Table 2. Various diversity indices from the Pleistocene West Pacific elasmobranch assemblages  
1186 showing high diversity of the present material. See Supplemental Table S1 for details of the data.

# Figure 1

Summary of the sampling sites.

A, overview of geological map of Taiwan (modified after Chen, 2016). B, geological map of Nuibu area, Chiayi (map extracted from National Geological Data Warehouse, Central Geological Survey, MOEA). Yellow stars = sampling sites (see Fig. 2B for details). C, stratigraphic correlation of the Western Foothills (modified after Chen, 2016). Liuchungchi Formation is indicated in yellow.

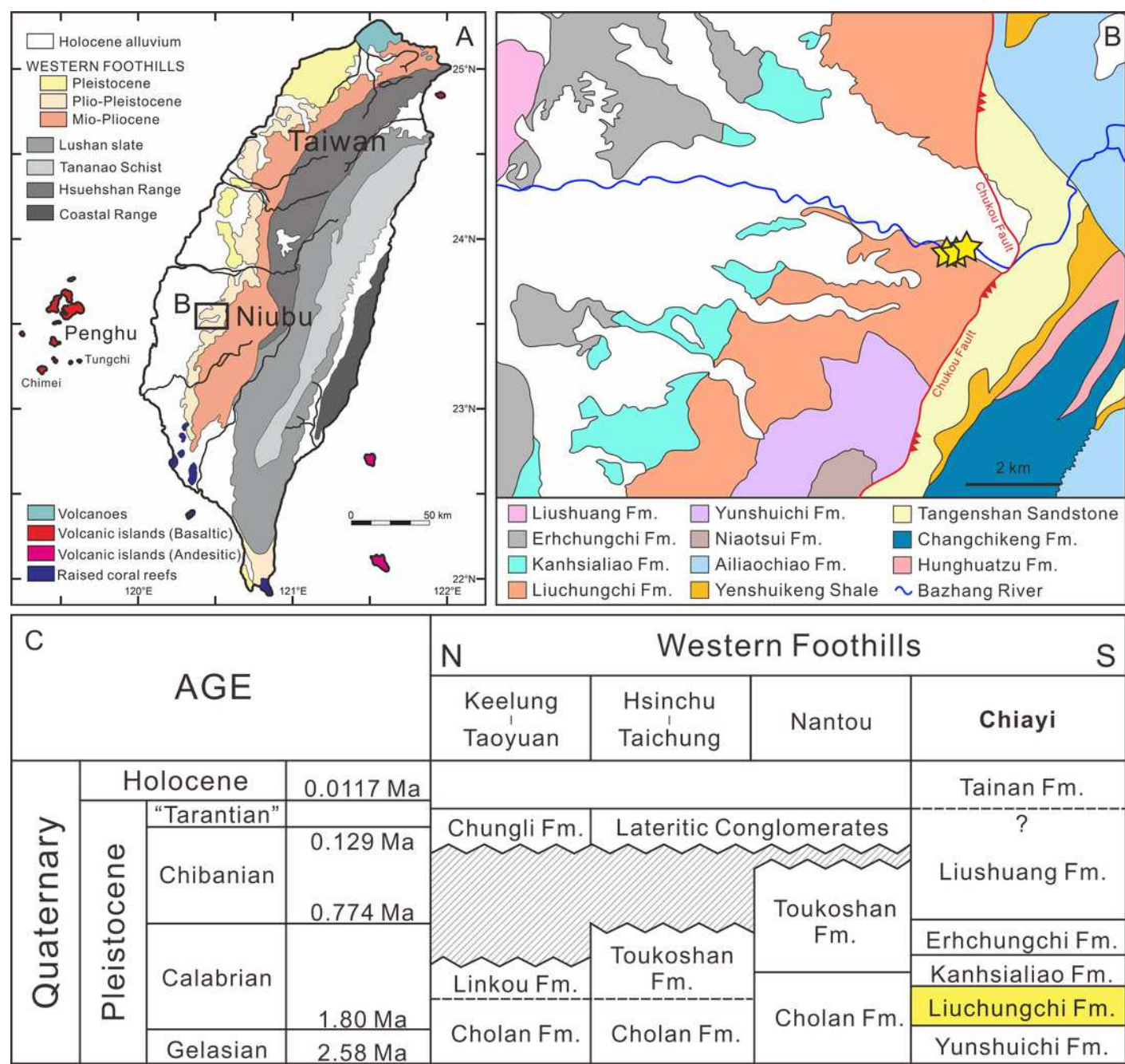


# Figure 2

A, stratigraphic column (modified after Huang, 2010). B, details of the sampling sites.

GPS coordinates: Site 1 = 23°26'23.4"N, 120°35'35.5"E; Site 2 = 23°26'22.6"N, 120°35'32.7"E; Site 3 = 23°26'23.5"N, 120°35'29.8"E.

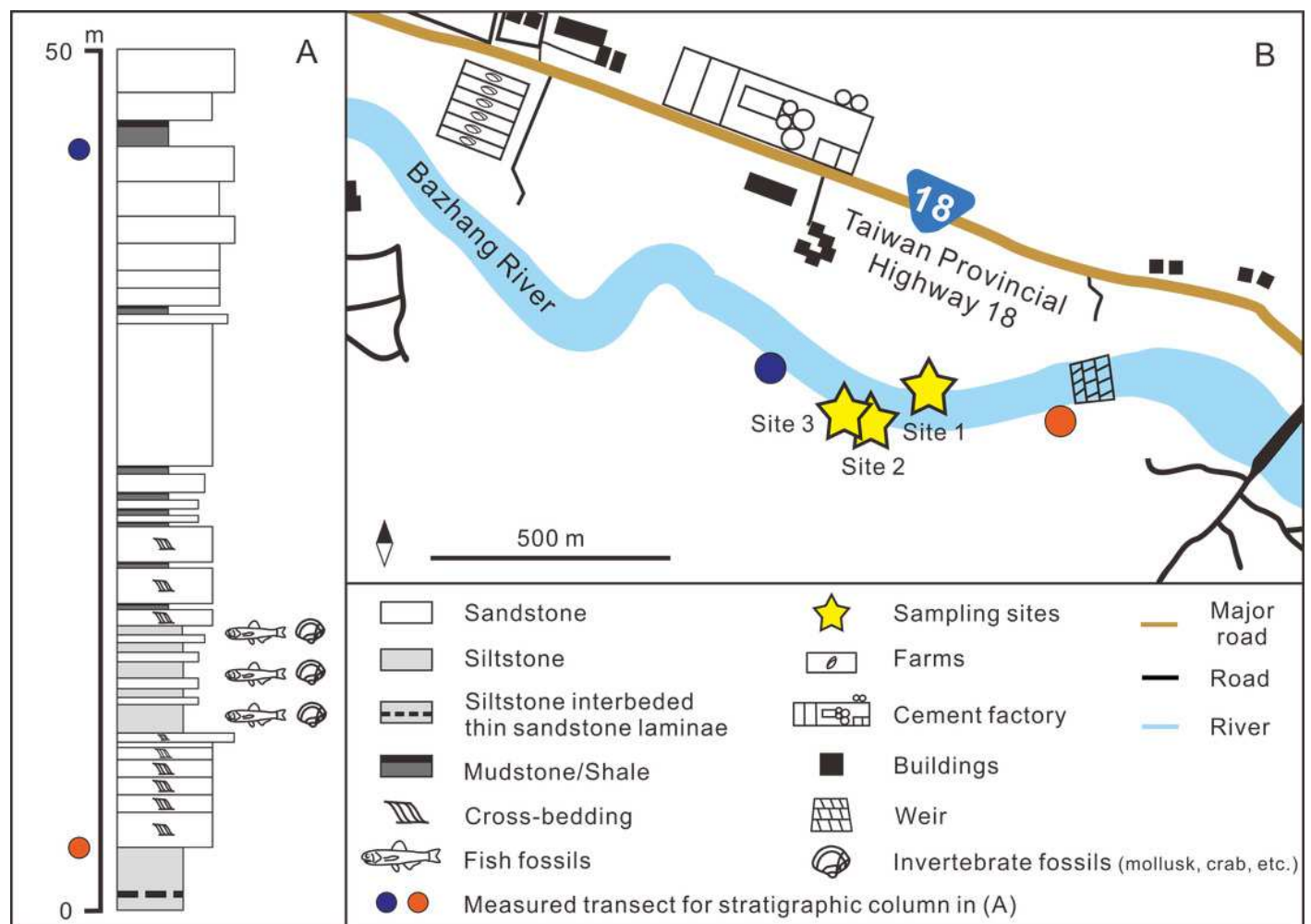


# Figure 3

Teeth of *Carcharias taurus* from the early Pleistocene, Liuchungchi Formation of Niubu, southern Taiwan.

A, B, ASIZF0100320; C-E, CMM F0204. A, C = lingual views; B, D = labial views; E = lateral view. Scale bar = 1 cm.



# Figure 4

Teeth of *Carcharodon carcharias* from the early Pleistocene, Liuchungchi Formation of Niubu, southern Taiwan.

A, B, ASIZF0100344; C, D, ASIZF0100337; E, F, ASIZF0100338; G, H, ASIZF0100336; I, J, ASIZF0100335; K, L, ASIZF0100339; M, N, ASIZF0100340; O, P, ASIZF0100324; Q, R, ASIZF0100328; S, T, ASIZF0100325; U, V, ASIZF0100326; W, X, ASIZF0100323. A, C, E, G, I, K, M, O, Q, S, U, W = lingual views; B, D, F, H, J, L, N, P, R, T, V, X = labial views. Scale bar = 1 cm.



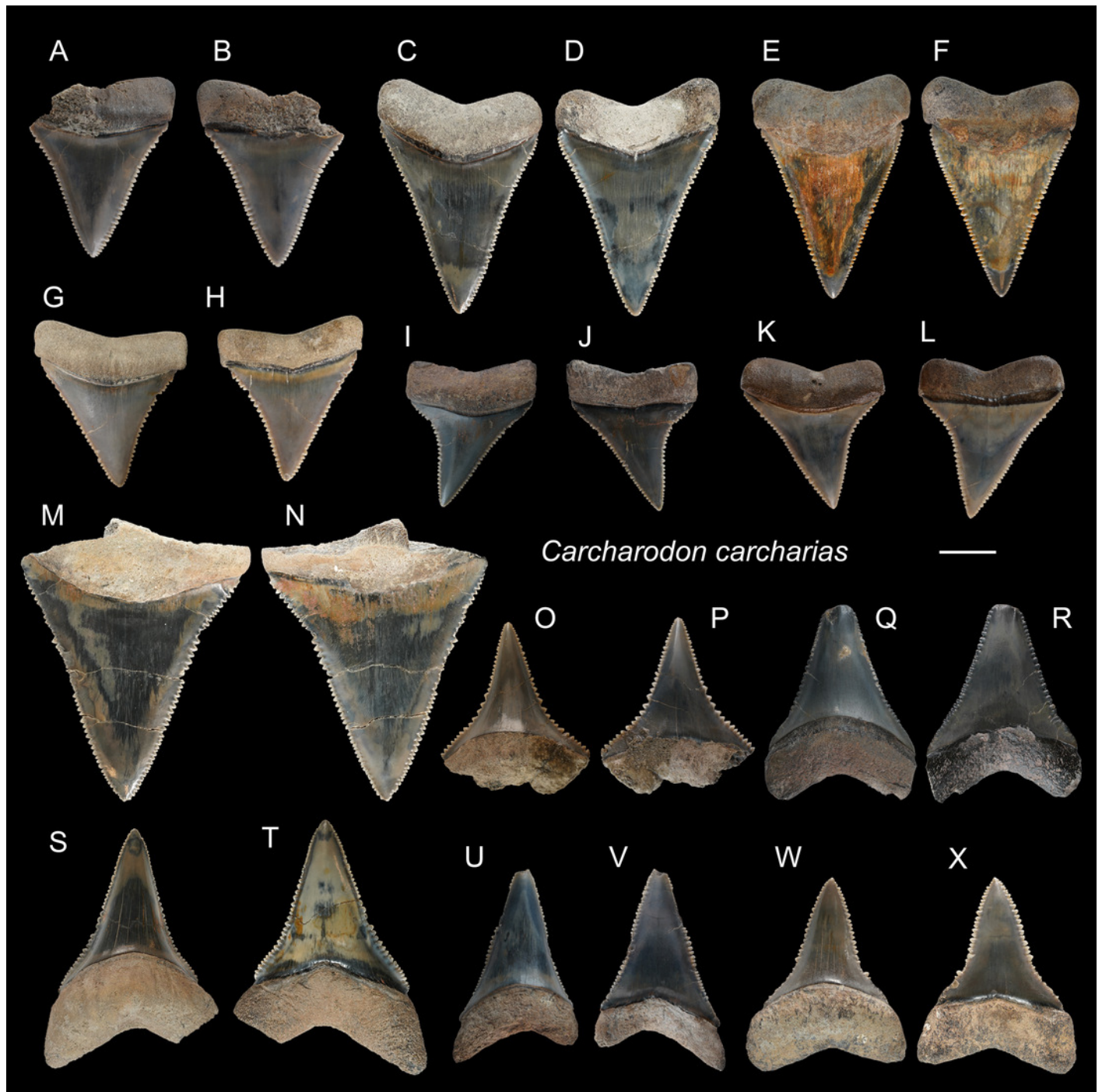




# Figure 5

Teeth of *Isurus oxyrinchus* from the early Pleistocene, Liuchungchi Formation of Niubu, southern Taiwan.

A-C, ASIZF0100317; D-F, ASIZF0100318; G, H, ASIZF0100321; I, J, CMM F0242. A, D, G, I = lingual views; B, E, H, J = labial views; C, F = lateral views. Scale bar = 1 cm.

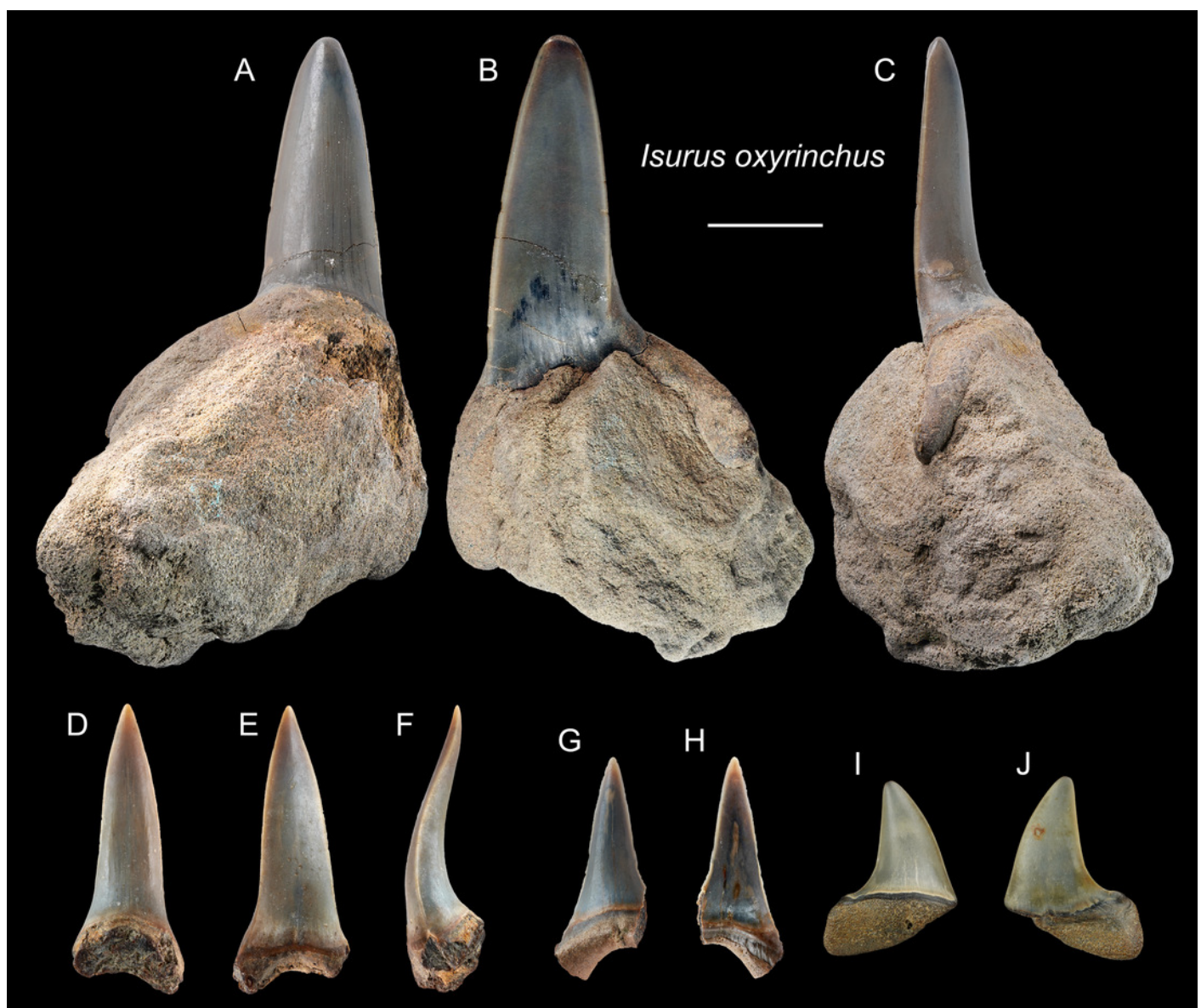


# Figure 6

Teeth of †*Hemipristis serra* from the early Pleistocene, Liuchungchi Formation of Niubu, southern Taiwan.

A, B, CMM F0232; C, D, ASIZF0100460; E, F, ASIZF0100461; G, H, ASIZF0100462. A, C, E, G = lingual views; B, D, F, H = labial views. Scale bars = 1 cm.

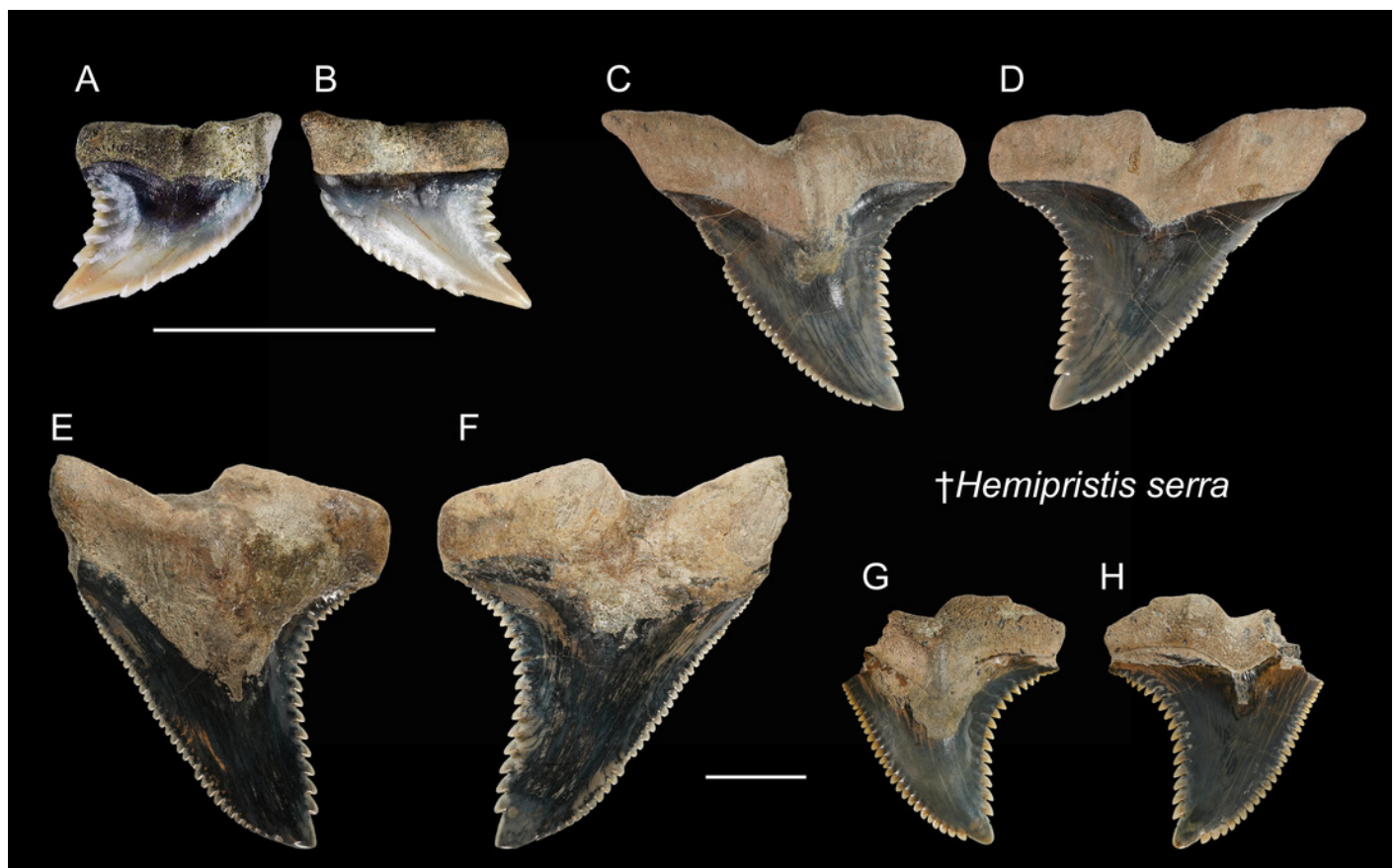


# Figure 7

Teeth of *Carcharhinus altimus* from the early Pleistocene, Liuchungchi Formation of Niubu, southern Taiwan.

A, B, ASIZF0100357; C, D, ASIZF0100359; E, F, CMM F0363; G, H, CMM F0293; I, J, CMM F0322; K, L, ASIZF 0100365. A, C, E, G, I, K = lingual views; B, D, F, H, J, L = labial views. Scale bar = 1 cm.

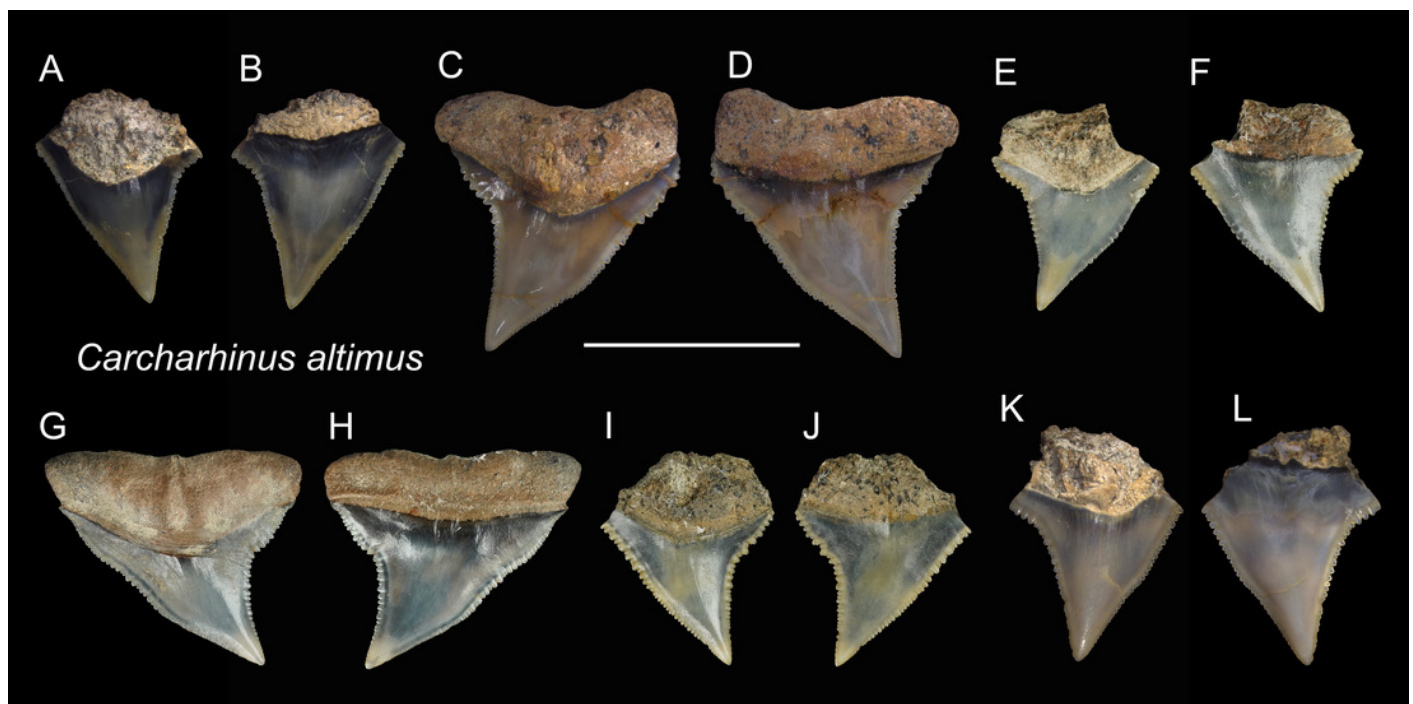


# Figure 8

Teeth of *Carcharhinus amboinensis* from the early Pleistocene, Liuchungchi Formation of Niubu, southern Taiwan.

A, B, CMM F0209; C, D, ASIZF0100368; E, F, ASIZF0100366; G, H, ASIZF0100369. A, C, E, G = lingual views; B, D, F, H = labial views. Scale bar = 1 cm.

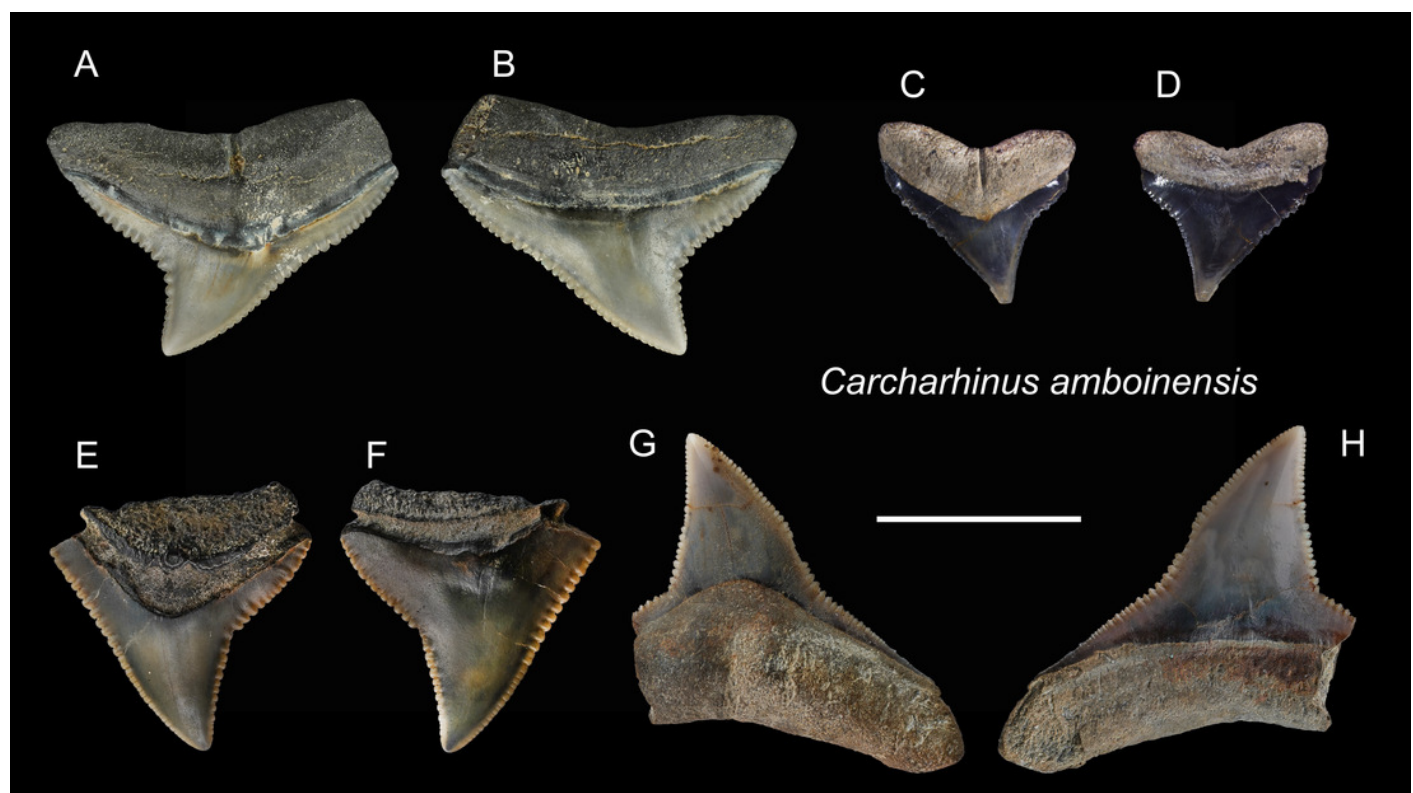




# Figure 9

Teeth of *Carcharhinus leucas* from the early Pleistocene, Liuchungchi Formation of Niubu, southern Taiwan.

A, B, ASIZF0100398; C, D, ASIZF0100397; E, F, ASIZF0100394; G, H, ASIZF0100411; I, J, ASIZF0100396; K, L, ASIZF 0100395; M, N, ASIZF0100400; O, P, ASIZF0100402; Q, R, ASIZF0100390. A, C, E, G, I, K, M, O, Q = lingual views; B, D, F, H, J, L, N, P, R = labial views. Scale bar = 1 cm.

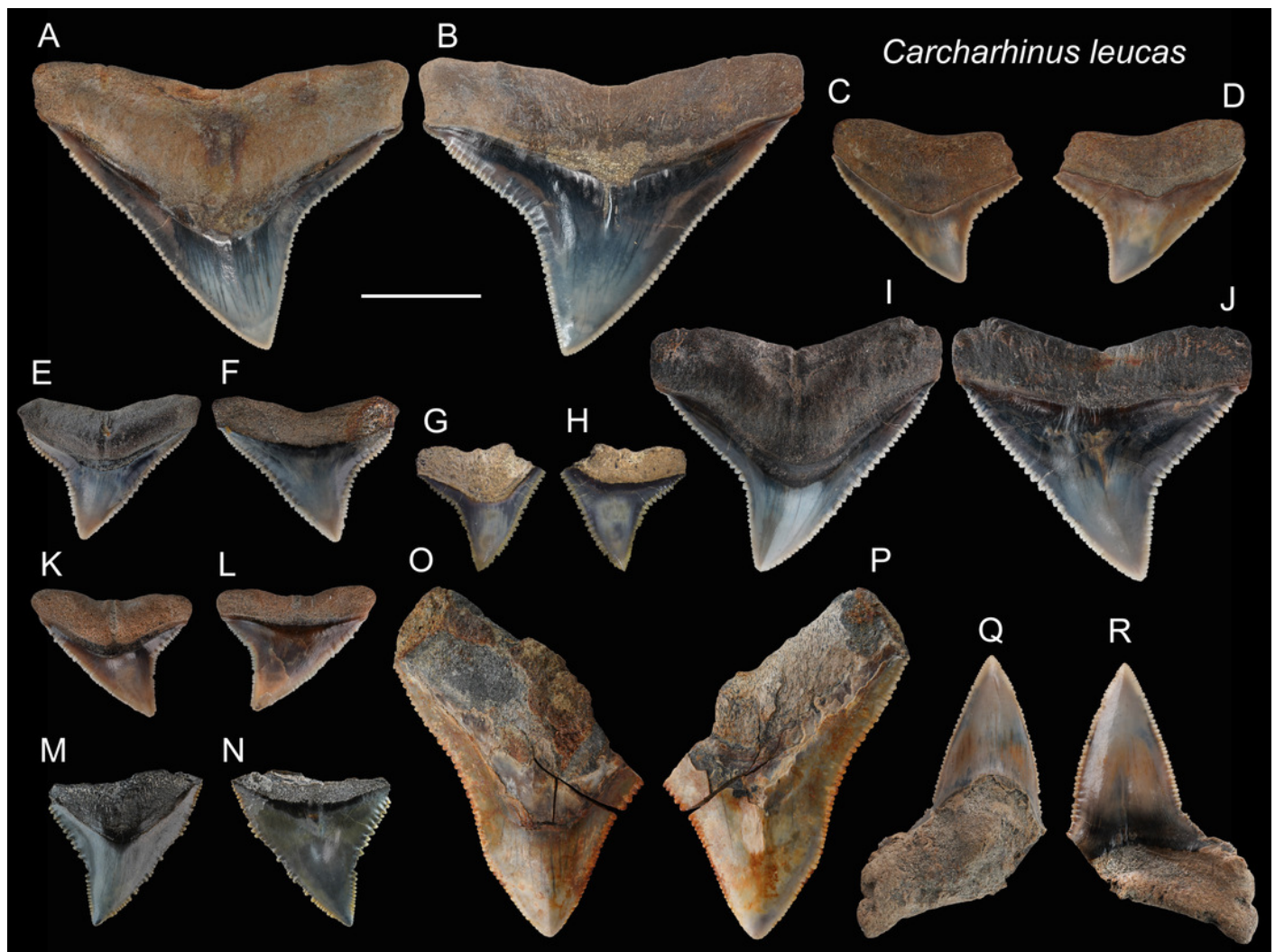


# Figure 10

Teeth of *Carcharhinus limbatus* from the early Pleistocene, Liuchungchi Formation of Niubu, southern Taiwan.

A, B, ASIZF0100470; C, D, ASIZF0100476; E, F, ASIZF0100469; G, H, ASIZF0100468; I, J, CMM F0236; K, L, CMM F0111; M, N, CMM F0237; O, P, CMM F0238. A, C, E, G, I, K, M, O = lingual views; B, D, F, H, J, L, N, P = labial views. Scale bar = 1 cm.

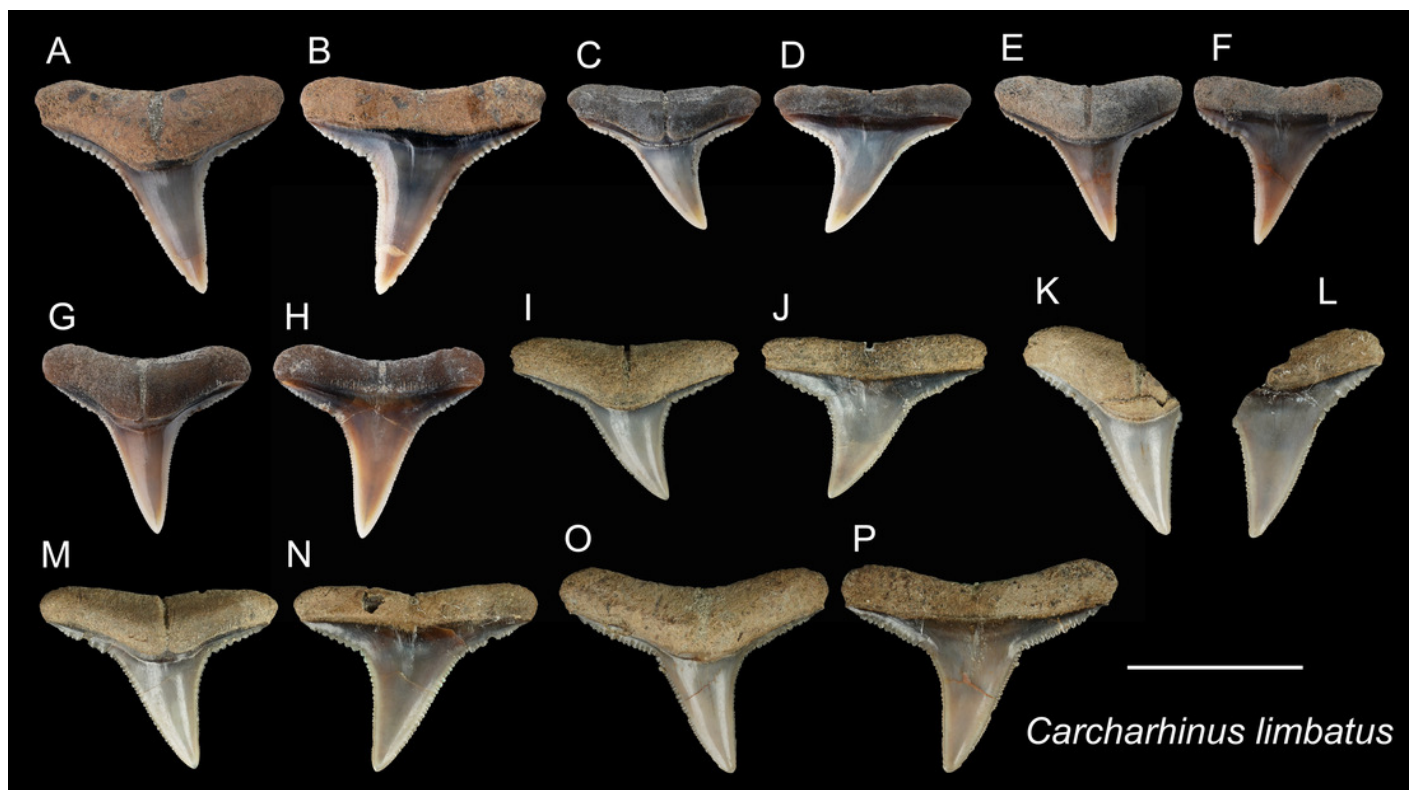


# Figure 11

Teeth of *Carcharhinus longimanus* from the early Pleistocene, Liuchungchi Formation of Niubu, southern Taiwan.

A, B, ASIZF 0100371; C, D, ASIZF0100376; E, F, ASIZF0100370; G, H, ASIZF0100377; I, J, ASIZF0100375; K, L, ASIZF0100378; M, N, ASIZF0100374; O, P, ASIZF0100373; Q, R, ASIZF0100392; S, T, ASIZF0100391. A, C, E, G, I, K, M, O, Q, S = lingual views; B, D, F, H, J, L, N, P, R, T = labial views. Scale bar = 1 cm.

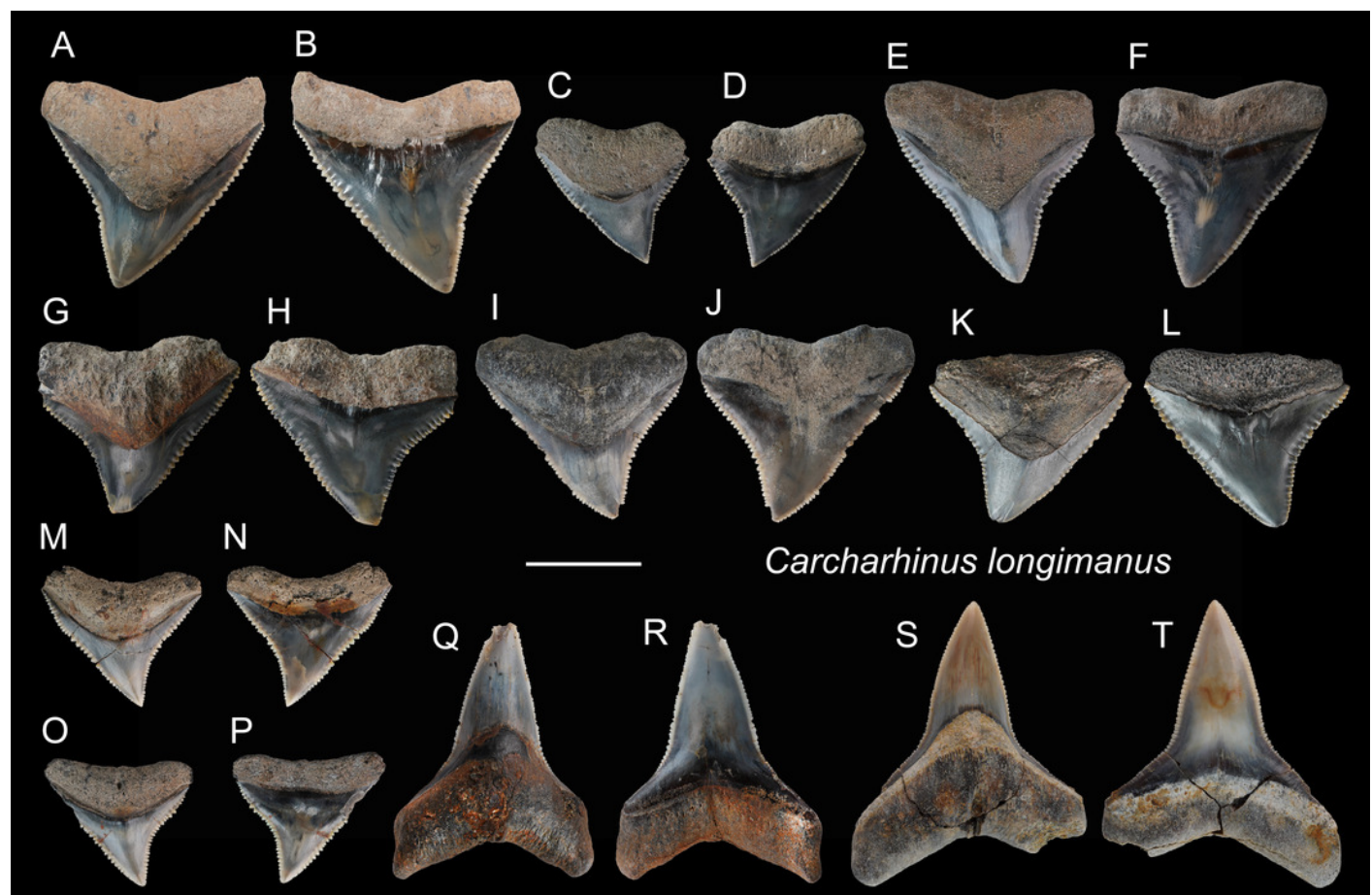




# Figure 12

Teeth of *Carcharhinus obscurus* from the early Pleistocene, Liuchungchi Formation of Niubu, southern Taiwan.

A, B, ASIZF0100372; C, D, ASIZF0100384; E, F, ASIZF0100385; G, H, ASIZF0100386; I, J, ASIZF0100388; K, L, ASIZF0100387; M, N, ASIZF0100383. A, C, E, G, I, K, M = lingual views; B, D, F, H, J, L, N = labial views. Scale bar = 1 cm.

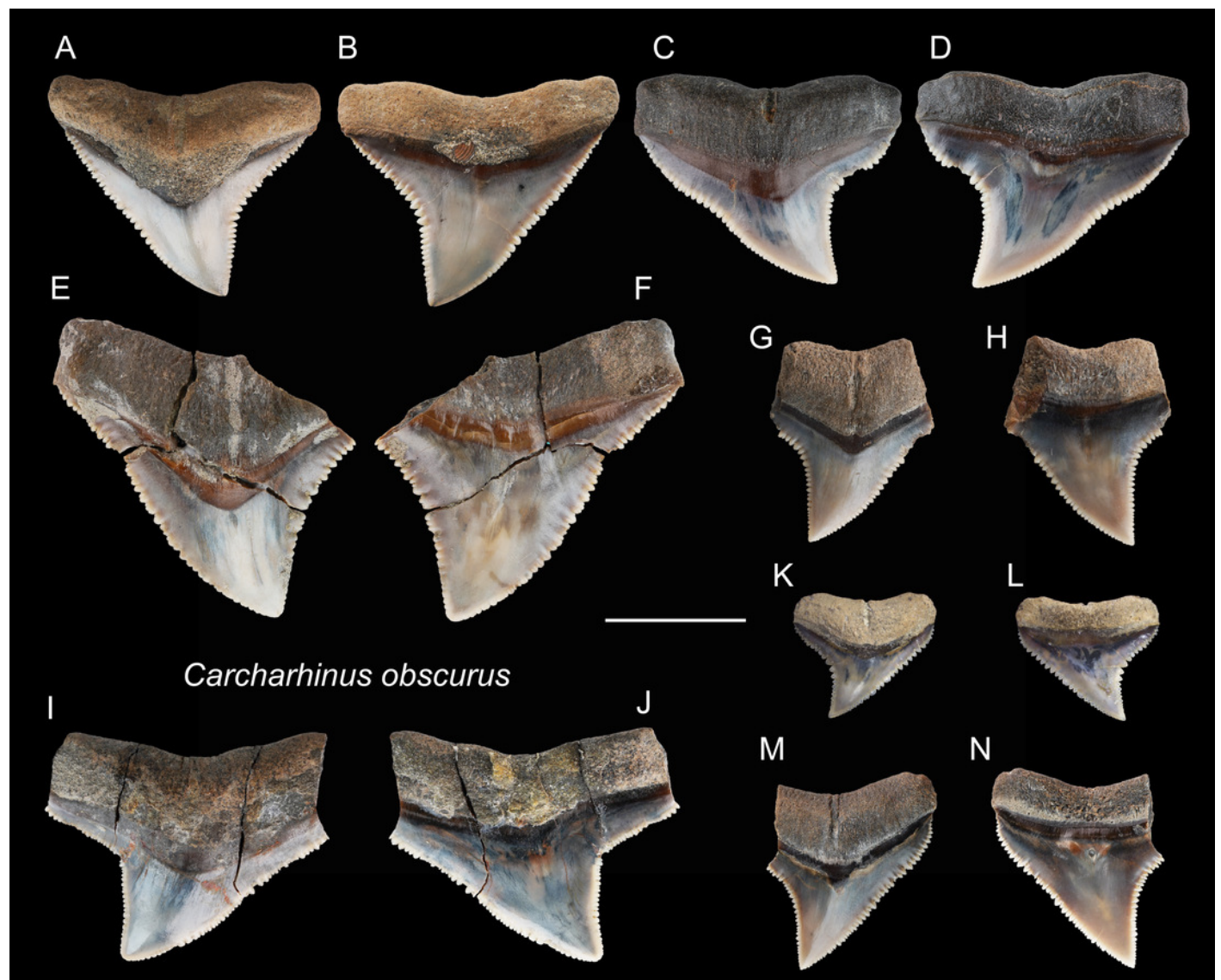




# Figure 13

Teeth of *Carcharhinus plumbeus* from the early Pleistocene, Liuchungchi Formation of Niubu, southern Taiwan.

A, B, ASIZF0100412; C, D, ASIZF0100406; E, F, ASIZF0100405; G, H, ASIZF0100410; I, J, ASIZF0100409; K, L, ASIZF0100408; M, N, ASIZF0100407. A, C, E, G, I, K, M = lingual views; B, D, F, H, J, L, N = labial views. Scale bar = 1 cm.

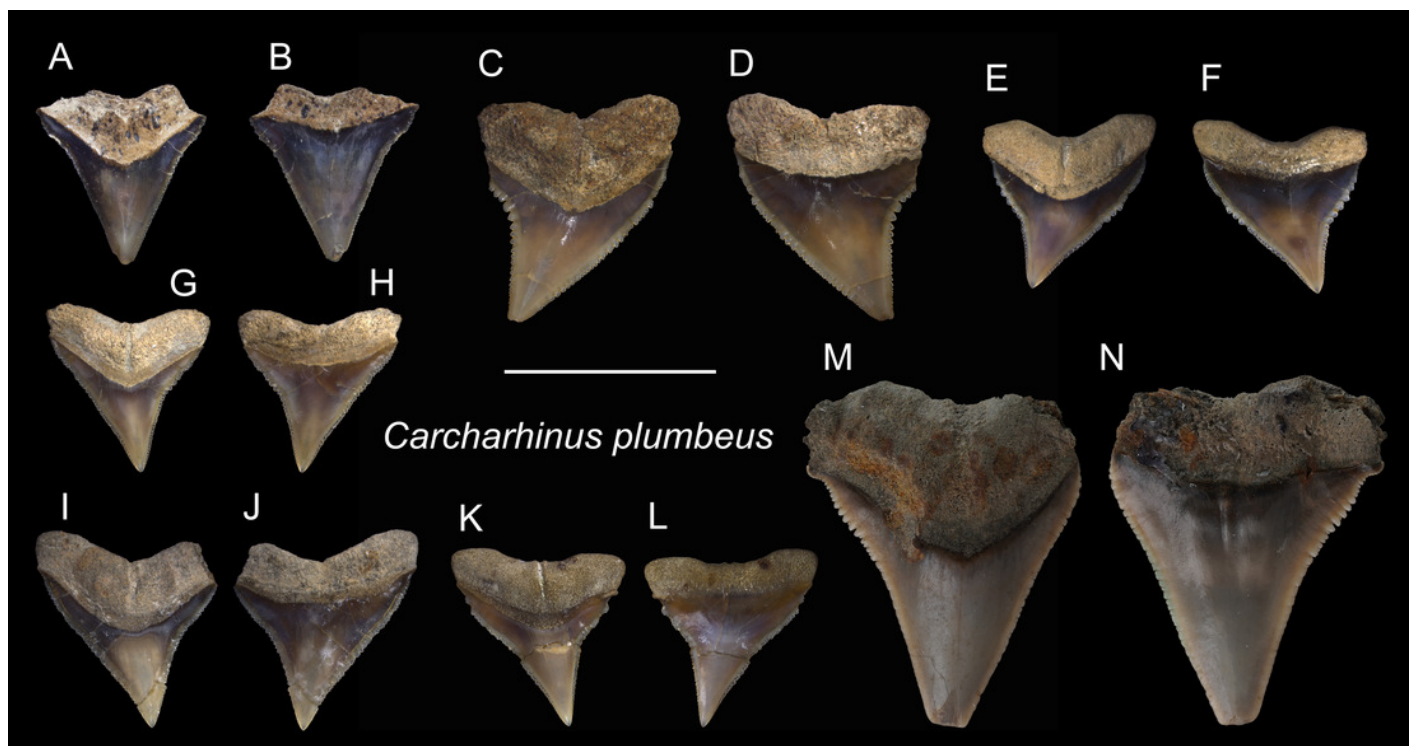


# Figure 14

Teeth of *Carcharhinus sorrah* from the early Pleistocene, Liuchungchi Formation of Niubu, southern Taiwan.

A, B, CMM F0129; C, D, CMM F0119; E, F, ASIZF0100418; G, H, CMM F0126; I, J, CMM F0135; K, L, CMM F0122; M, N, CMM F0140. A, C, E, G, I, K, M = lingual views; B, D, F, H, J, L, N = labial views. Scale bar = 1 cm.

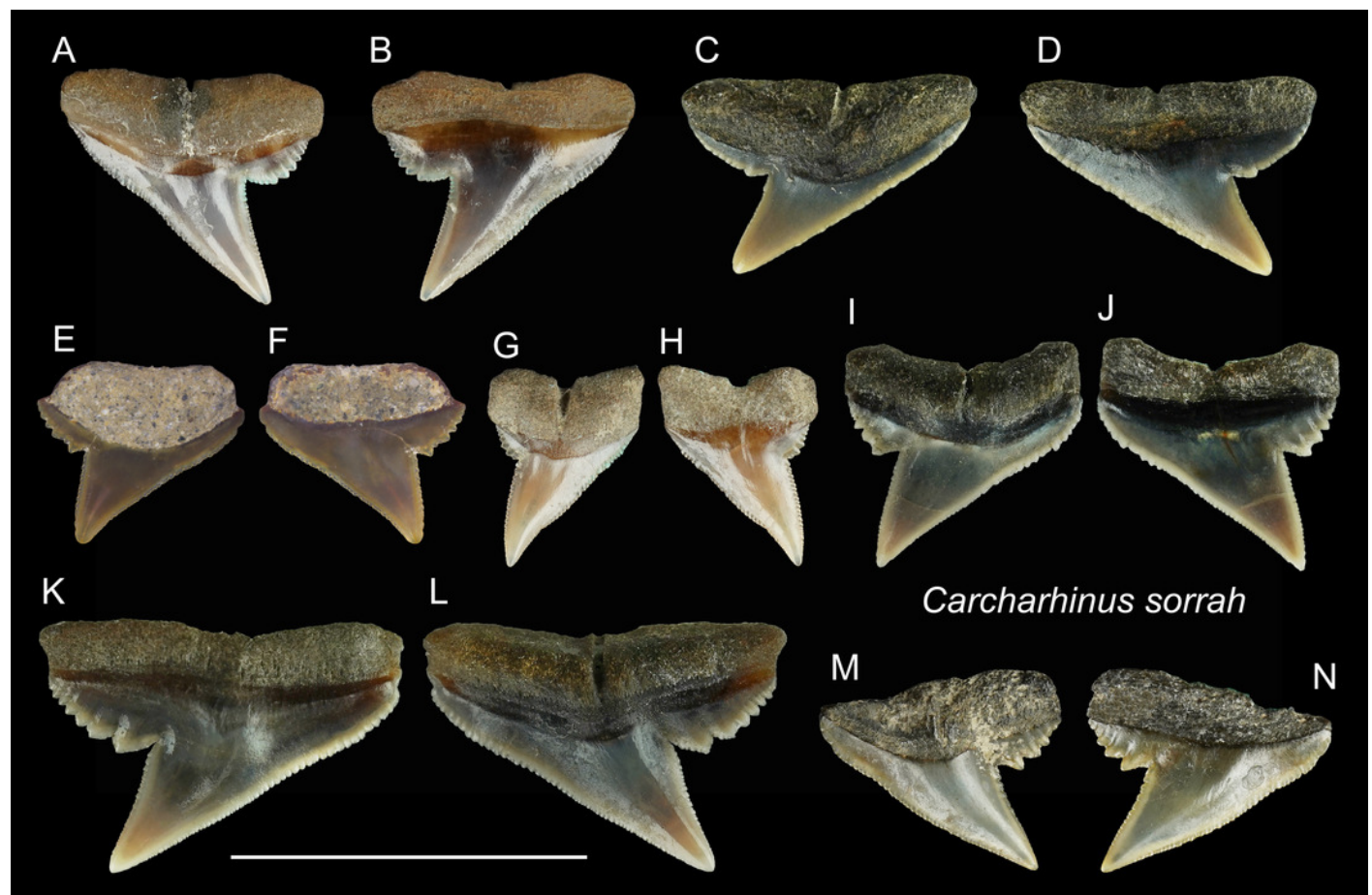


# Figure 15

Teeth of *Carcharhinus tjtjt* from the early Pleistocene, Liuchungchi Formation of Niubu, southern Taiwan.

A, B, ASIZF0100415; C, D, ASIZF0100414; E, F, CMM F0116; G, H, ASIZF0100413; I, J, ASIZF0100417; K, L, ASIZF0100416; M, N, CMM F0323; O, P, CMM F0324. A, C, E, G, I, K, M, O = lingual views; B, D, F, H, J, L, N, P = labial views. Scale bar = 1 cm.

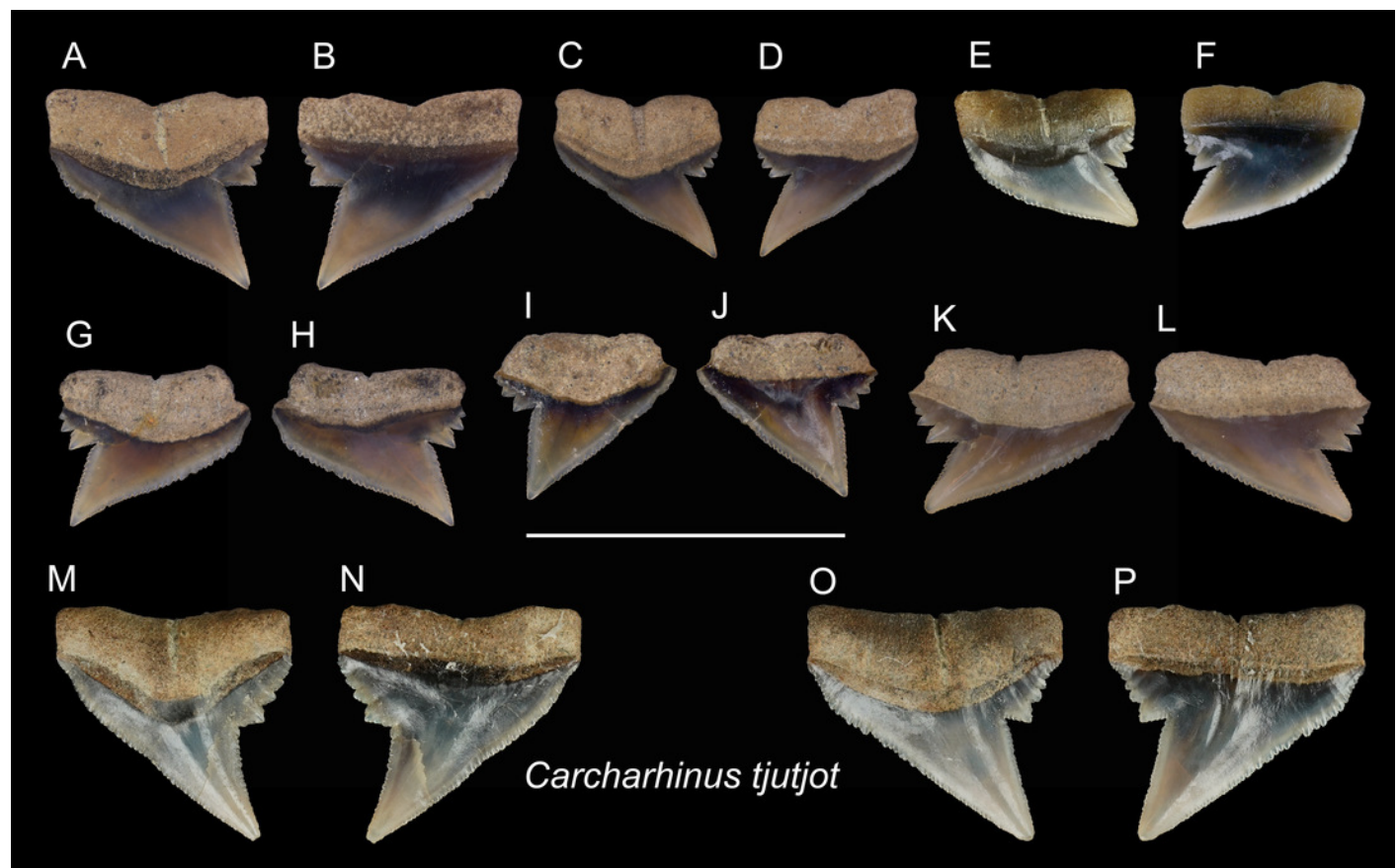


# Figure 16

Teeth of *Rhizoprionodon acutus* from the early Pleistocene, Liuchungchi Formation of Niubu, southern Taiwan.

A, B, ASIZF0100463; C, D, CMM F0120; E, F, CMM F0121; G, H, CMM F0131; I, J, ASIZF0100464. A, C, E, G, I = lingual views; B, D, F, H, J = labial views. Scale bar = 1 cm.

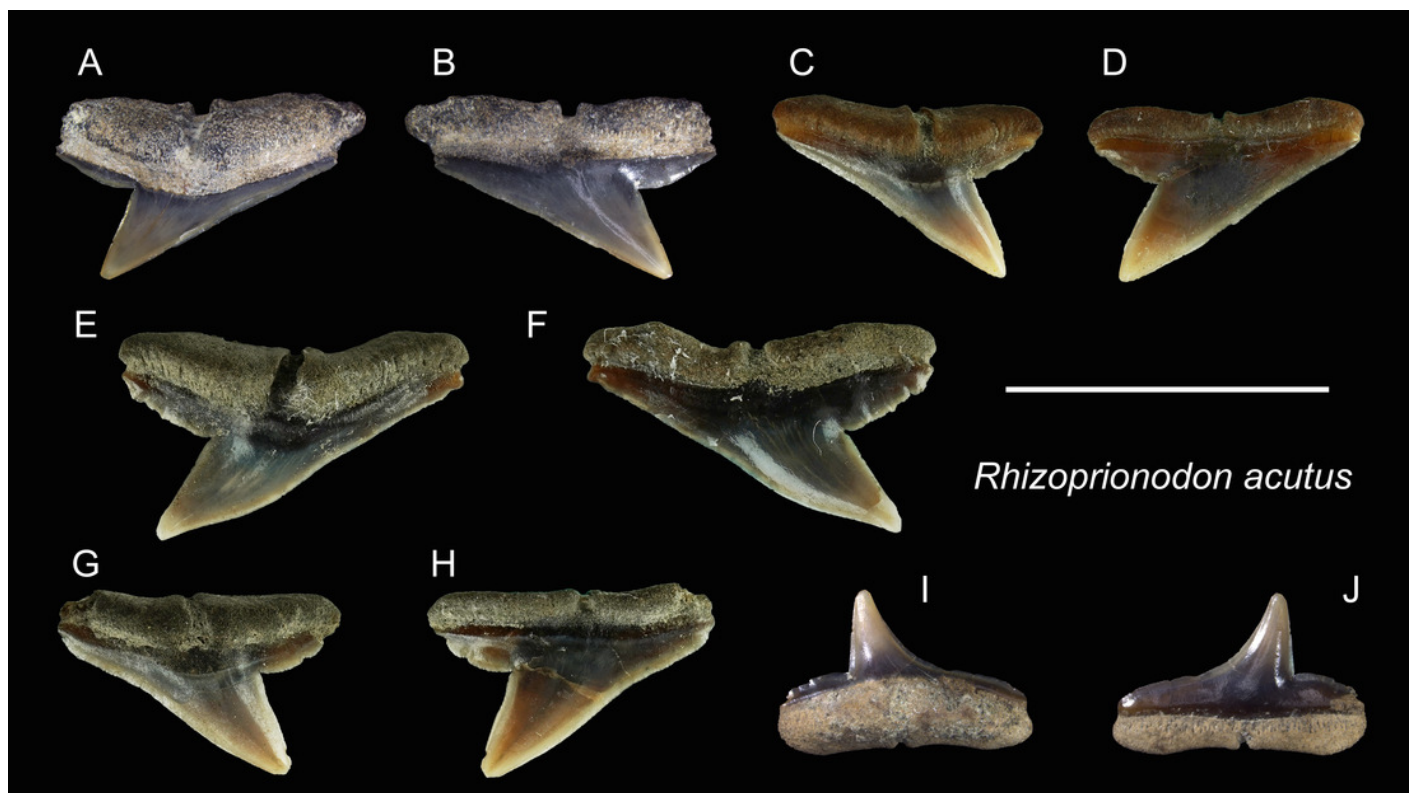




# Figure 17

Teeth of *Galeocerdo cuvier* and *Sphyrna lewini* from the early Pleistocene, Liuchungchi Formation of Niubu, southern Taiwan.

A–H, *Galeocerdo cuvier*; A, B, CMM F0245; C–E, CMM F0215; F–H, ASIZF0100459. I–L, *Sphyrna lewini*; I, J, CMM F0235; K, L, CMM F0312. A, C, F, I, K = lingual views; B, D, G, J, L = labial views; E, H = details of secondary serrations. Scale bars = 1 cm.

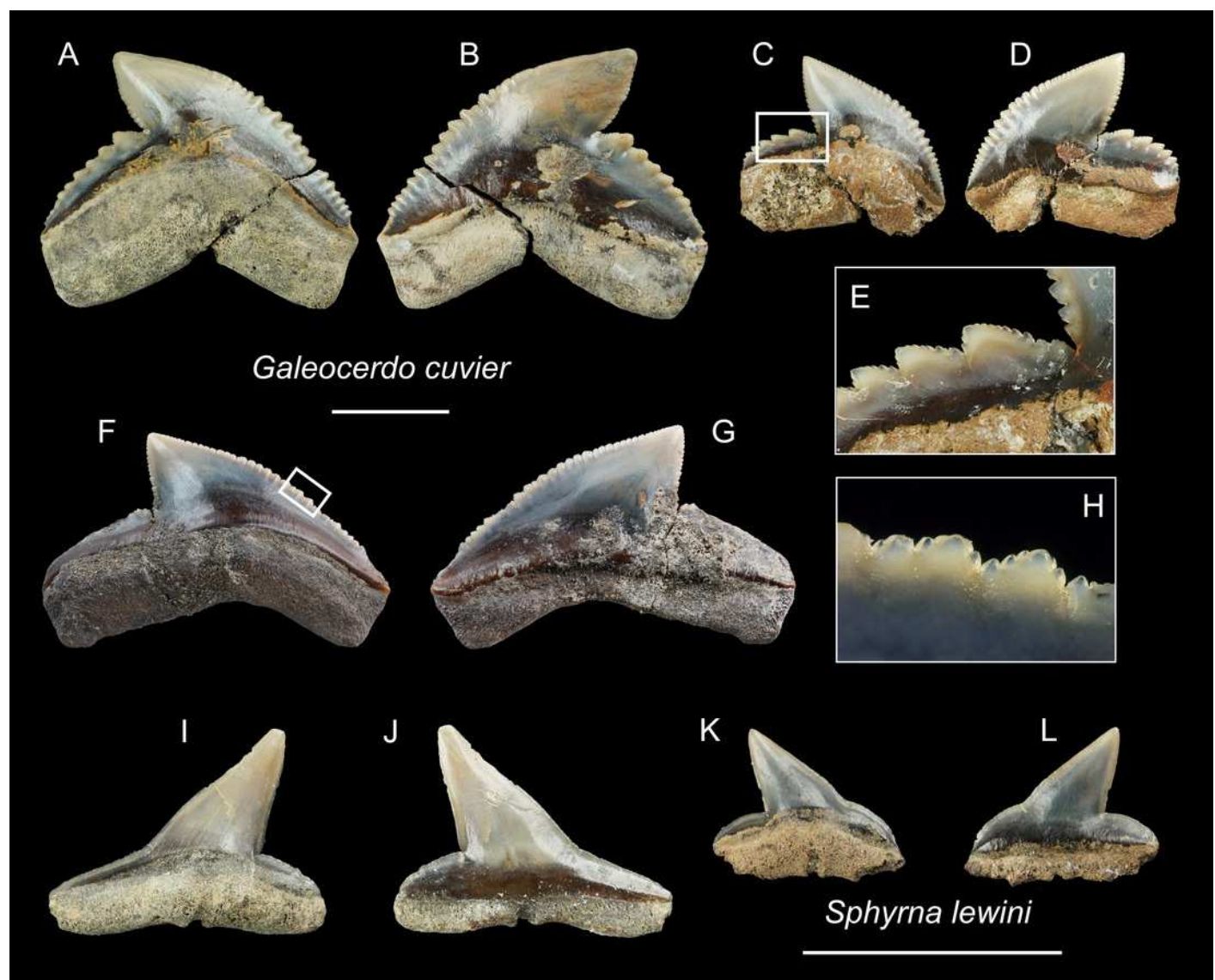


# Figure 18

Teeth of *Dasyatidae* indet. from the early Pleistocene, Liuchungchi Formation of Niubu, southern Taiwan.

A-D, ASIZF0100590; E-H, ASIZF0100591. A, E = labial views; B, F = basal views; C, G = occlusal views; D, H = lateral views. Scale bar = 5 mm.

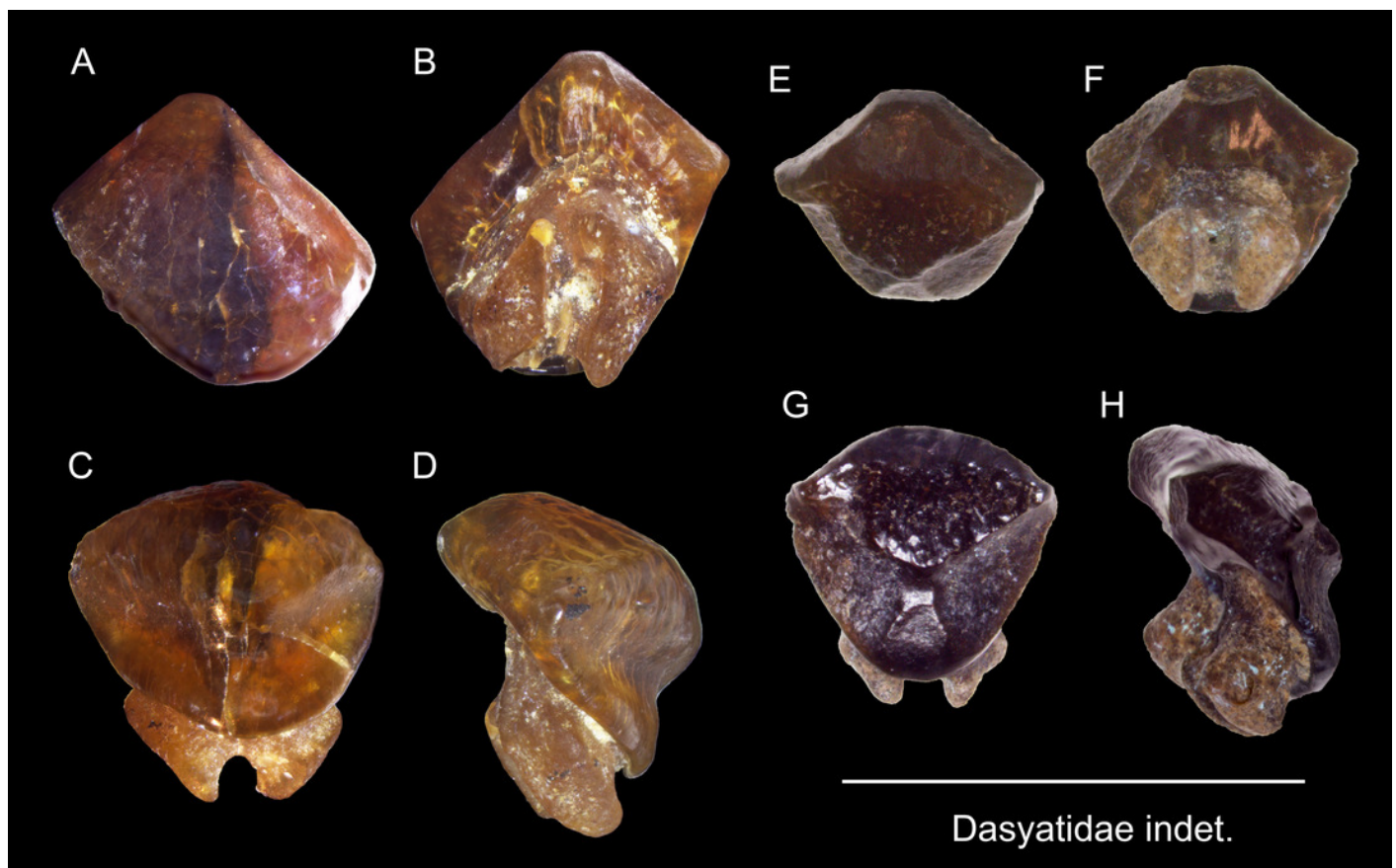


# Figure 19

Teeth of *Aetobatus* sp. from the early Pleistocene, Liuchungchi Formation of Niubu, southern Taiwan.

A, B, CMM F2854; C, D, CMM F2850; E, F, CMM F0408; G, H, ASIZF0100549. A, C, E, G = occlusal views; B, D, F, H = basal views. Scale bar = 1 cm.

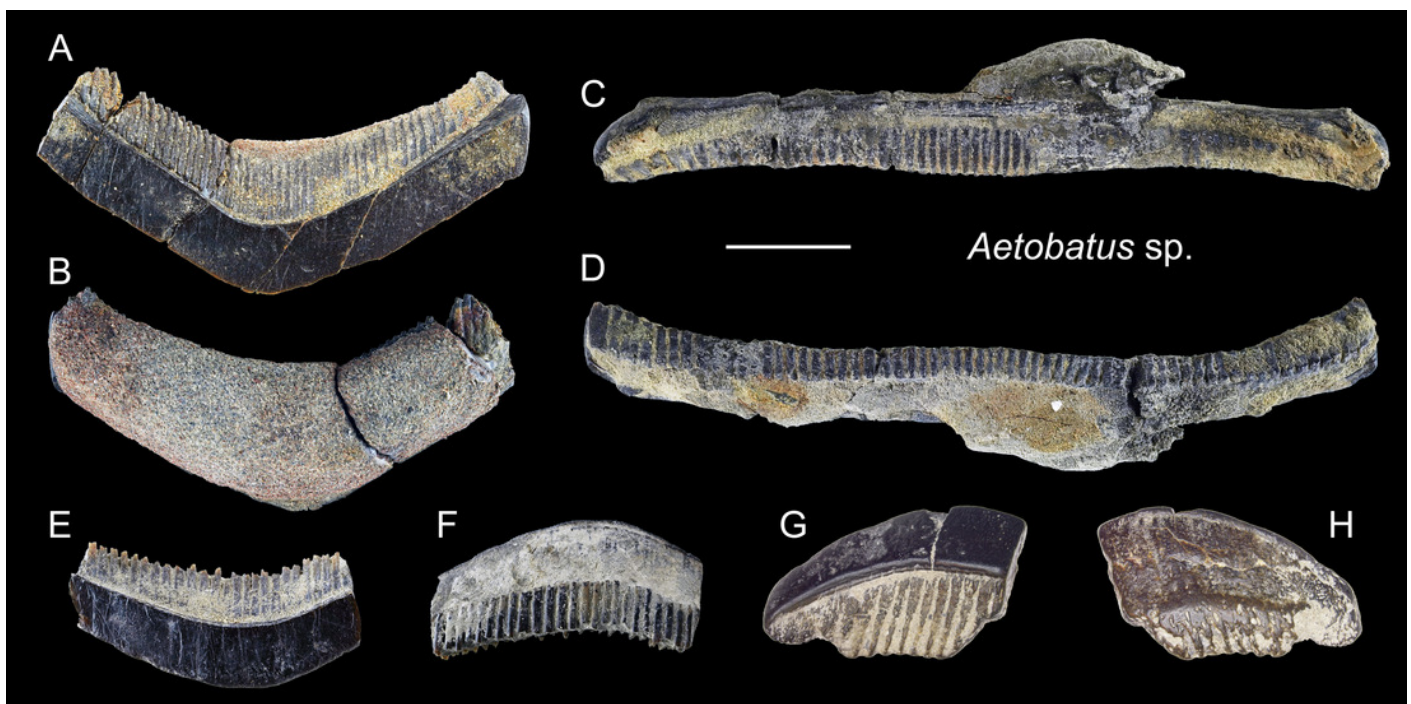




# Figure 20

Teeth of *Myliobatis* sp. from the early Pleistocene, Liuchungchi Formation of Niubu, southern Taiwan.

A-D, ASIZF0100582; E-H, ASIZF0100587; I-L, ASIZF0100586; M, N, CMM F0395; O, P, CMM F2855; Q, R, CMM F0393; S, T, CMM F0398. A, E, I, M, O, Q, S = occlusal views; B, F, J, N, P, R, T = basal views; C, G, K = lingual views; D, H, L = labial views. Scale bars = 1 cm.

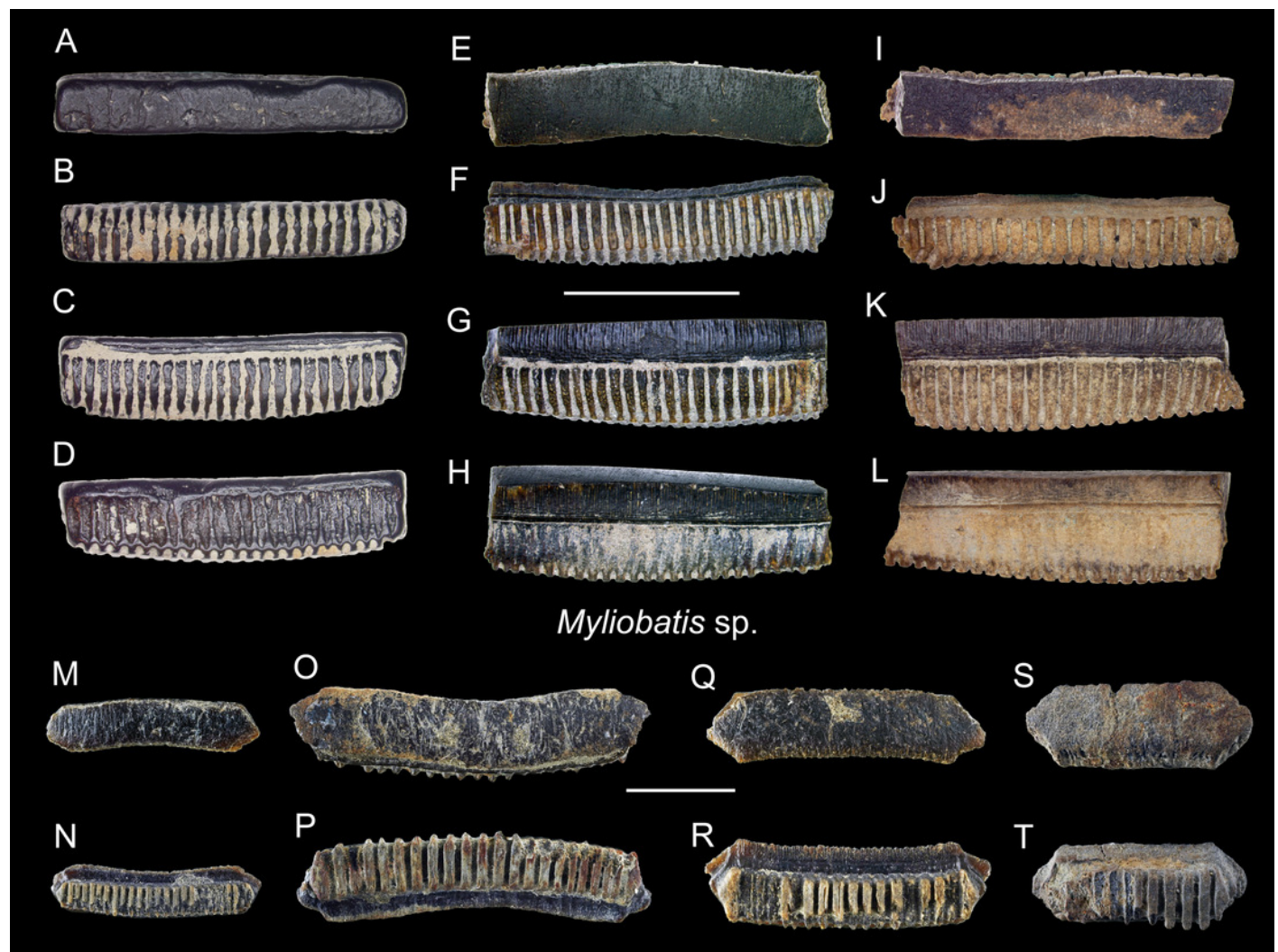




**Table 1**(on next page)

Elasmobranchs from the early Pleistocene Liuchungchi Formation of Niubu, southern Taiwan.

1 Table 1. Elasmobranchs from the early Pleistocene Liuchungchi Formation of Niubu, southern Taiwan.  
2

Order	Family	Taxa	ASIZF	CMM	NTM	Total
Lamniformes	Carchariidae	<i>Carcharias taurus</i>	1	1		2
Lamniformes	Lamnidae	<i>Carcharodon carcharias</i>	28	25	2	55
Lamniformes	Lamnidae	<i>Isurus oxyrinchus</i>	4	1	1	6
Carcharhiniformes	Hemigaleidae	† <i>Hemipristis serra</i>	3	3	1	7
Carcharhiniformes	Carcharhinidae	<i>Carcharhinus altimus</i>	5	10	2	17
Carcharhiniformes	Carcharhinidae	<i>Carcharhinus amboinensis</i>	3	2		5
Carcharhiniformes	Carcharhinidae	<i>Carcharhinus leucas</i>	17	53	1	71
Carcharhiniformes	Carcharhinidae	<i>Carcharhinus limbatus</i>	16	21	3	40
Carcharhiniformes	Carcharhinidae	<i>Carcharhinus longimanus</i>	18	16	2	36
Carcharhiniformes	Carcharhinidae	<i>Carcharhinus obscurus</i>	9	15	1	25
Carcharhiniformes	Carcharhinidae	<i>Carcharhinus plumbeus</i>	8	42	1	51
Carcharhiniformes	Carcharhinidae	<i>Carcharhinus sorrah</i>	1	10		11
Carcharhiniformes	Carcharhinidae	<i>Carcharhinus tjtjt</i>	5	14		19
Carcharhiniformes	Carcharhinidae	<i>Carcharhinus</i> spp.	88	110	10	208
Carcharhiniformes	Carcharhinidae	<i>Rhizoprionodon acutus</i>	2	6		8
Carcharhiniformes	Galeocerdonidae	<i>Galeocerdo cuvier</i>	1	5	1	7
Carcharhiniformes	Sphyrnidae	<i>Sphyrna lewini</i>		2		2
Myliobatiformes	Dasyatidae	Dasyatidae indet.	2			2
Myliobatiformes	Aetobatidae	<i>Aetobatus</i> sp.	32	22	4	58
Myliobatiformes	Myliobatidae	<i>Myliobatis</i> sp.	9	20	1	30
Indet.	Indet.	Indet.	25	12		37
Total			277	390	30	697

3

## **Table 2**(on next page)

Various diversity indices from the Pleistocene West Pacific elasmobranch assemblages showing high diversity of the present material.

See Supplemental Table S1 for details of the data.

- 1 Table 2. Various diversity indices from the Pleistocene West Pacific elasmobranch assemblages showing high diversity of the present
- 2 material. See Supplemental Table S1 for details of the data.

Location	Age	Species richness	Shannon	Simpson	Fisher's alpha	Reference
Taiwan	early Pleistocene	20	2.4	0.9	3.9	Our study
Sulawesi	Pleistocene	6	1.6	0.8	2.0	Hooijer, 1954
Java	Pleistocene	4	0.9	0.5	1.4	Koumans, 1949
Java	Plio-Pleistocene	11	1.7	0.7	2.9	Yudha et al., 2018
Central Japan	early Pleistocene	2	0.5	0.3	1.2	Karasawa, 1989
Central Japan	middle Pleistocene	14	2.2	0.9	6.0	Kawase & Nishimatsu, 2016
Eastern Japan	Pleistocene	14	2.3	0.9	4.6	Tanaka & Taru, 2022

3